EVALUATION OF ZINC TOXICITY USING NEURONAL NETWORKS ON MICROELECTRODE ARRAYS: RESPONSE QUANTIFICATION AND ENTRY PATHWAY ANALYSIS.

Maryam Parviz, B.S., M.S.

Dissertation Prepared for the Degree of

DOCTOR OF PHILOSOPHY

UNIVERSITY OF NORTH TEXAS

August 2007

APPROVED:

Guenter W. Gross, Major Professor
Kent Chapman, Committee Member
Jannon Fuchs, Committee Member
Kamashki Gopal, Committee Member
DiAnna Hynds, Committee Member
Harris Schwark, Committee Member
Sam Atkinson, Chair of the Department of Biological Sciences
Sandra L. Terrell, Dean of the Robert B. Toulouse School of Graduate Studies

Parviz, Maryam, Evaluation of zinc toxicity using neuronal networks on microelectrode arrays: response quantification and entry pathway analysis. Doctor of Philosophy (Molecular Biology), August 2007, 81 pp., 8 tables, 25 figures, references, 92 titles.

Murine neuronal networks, derived from embryonic frontal cortex (FC) tissue grown on microelectrode arrays, were used to investigate zinc toxicity at concentrations ranging from 20 to 2000 μM total zinc acetate added to the culture medium. Continual multi-channel recording of spontaneous action potential generation allowed a quantitative analysis of the temporal evolution of network spike activity generation at specific zinc acetate concentrations. Cultures responded with immediate concentration-dependent excitation lasting from 5 to 50 min, consisting of increased spiking and enhanced, coordinated bursting. This was followed by irreversible activity decay. The time to 50% and 90% activity loss was concentration dependent, highly reproducible, and formed linear functions in log–log plots. Network activity loss generally preceded morphological changes. 20% cell swelling was correlated with 50% activity loss. Cultures pretreated with the $GABA_A$ receptor antagonists bicuculline (40 μM) and picrotoxin (1 mM) lacked the initial excitation phase. This suggests that zinc-induced excitation may be mediated by interfering with GABA inhibition. Partial network protection was achieved by stopping spontaneous activity with either tetrodotoxin (200 nM) or lidocaine (250 μM). However, recovery was not complete and slow deterioration of network activity continued over 6 hrs. Removal of zinc by early medium changes showed irreversible, catastrophic network failure to develop in a concentration-dependent time window between 50% and 90% activity loss. Investigation of entry

routes suggested the L-type but not N-type calcium channels to be the main entry pathway for zinc. Data are presented implicating the chloride channel to be an additional entry route.

ACKNOWLEDGEMENTS

I am grateful for the almost daily support given to me by Professor Gross and for the encouragement and specific assistance provided at different times by the members of my committee. In addition, I am grateful for the excellent cell culture support by Nga Nguyen and Cara Santa Maria, as well as for the MEA fabrication effort under the direction of Ahmet Ors. Also I greatly thank my wonderful parents and sister for their help and support. Financial support was provided by The Texas Advanced Technology Program through a grant to Prof. Gross and by the Charles Bowen Memorial Endowment to the Center for Network Neuroscience.

TABLE OF CONTENTS

LIST OF TABLES

Page

LIST OF FIGURES

Page

CHAPTER 1

INTRODUCTION

1.1 Zinc and the Nervous System

Zinc is heterogeneously distributed throughout the brain, varying over a five-fold range from 26–40 ppm (369-568 μM) in cortical gray matter to 136–145 ppm (1.931-2.059 mM) in hippocampal mossy fibers (Choi and Koh, 1998). Zinc can be released into the synapse to modulate the activity of various neurotransmitter receptors. For example, zinc inhibits N-methyl-d-aspartate (NMDA) and γ-aminobutyric acid (GABA) receptors, and potentiates α-amino-5-hydroxy- 3-methyl-4-isoxazole propionic acid (AMPA) receptors (Harrison and Gibbons, 1994; Smart et al*.,* 1994). Additionally, zinc inhibits transporter-mediated glutamate uptake (Vandenberg et al*.,* 1998) and, depending on concentration, can inhibit or potentiate glycine receptors (Han & Wu, 1999; Spiridon et al.,1998). While synaptic zinc may be important for normal neural function, it is also known that zinc is toxic to neurons. Studies in animal models suggest that endogenous zinc mediates neurodegeneration resulting from ischemia (Koh et al*.,* 1996) and seizure (Suh et al., 1996). Numerous reports have shown that zinc is toxic to cultured neurons (Choi et al., 1988, 1992; Chen and Liao, 2003; Manev et al., 1997; Weiss et al*.,* 2000). Pharmacological approaches confirmed that zinc entered neurons and that such increases in intracellular free zinc resulted in neurotoxicity (Canzoniero et al., 1999; Sensi et al., 1997). Studies using zinc-sensitive fluorophores to directly measure increased intracellular zinc suggest that this divalent ion enters neurons through a number of calcium-permeable pathways: glutamate receptors, voltage-gated

calcium channels, and Na^{+}/Ca^{++} exchangers all permit zinc influx (Cheng and Reynolds, 1998; Colvin et al., 2000; Marin et al., 2000; Sensi et al., 1997; Sheline et al., 2002). In addition, some plasma membrane transporters may mediate accumulation of zinc (Colvin, 1998; Colvin et al., 2003). While zinc neurotoxicity has been established, and zinc-sensitive fluorophores have been used to measure intracellular zinc, it is important to note that few reports have demonstrated a quantitative relationship between zinc and zinc-mediated neurotoxicity (Canzoniero et al., 1999; Sensi et al., 1999). Also, early emphasis on excitotoxicity, that required examination of zinc effects in the presence of high concentrations of potassium, has dominated these studies and only limited information is available on zinc toxicity in normal physiological media. While the mechanisms by which increased intracellular zinc kills neurons remain unclear, it has been suggested that increased intracellular zinc may result in mitochondrial impairment and generation of reactive oxygen species (Dineley et al., 2003; Kim et al., 1999; Sensi et al., 1999).

1.2 Zinc Absorption and Excretion.

Adults in North America tend to generally consume 8 – 15 mg of zinc per day via their dietary intake (IOM, 2001). Under a normal diet, zinc absorption ranges from 26 – 33% of this exposure level (Sandstrom and Abrahamson, 1989; Knudsen et al., 1995; Hunt et al., 1998) whereas, fasting results in higher zinc absorption, 68 – 81% (Istfan et al., 1983; Sandstrom and Abrahamson, 1989). Zinc is mainly absorbed in the small intestine of the digestive tract. Studies in rats have suggested that 60% absorption occurs in the duodenum (Methfessel and Spencer, 1973; Davies, 1980), 30% in the

ileum, 8% in the jejunum, and 3% through the colon and cecum (Davies, 1980). Although, in more recent studies including human subjects (Lee et al., 1989), a greater rate of transport has been suggested across the jejunum than any other intestinal segment. The quantitative significance of the different intestinal segments is not yet clearly defined; however the fact that gastrointestinal absorption of zinc is biphasic is already well established, with a rapid phase occurring initially followed by a saturable slow phase (Davies, 1980; Gunshin et al., 1991).

Zinc absorption occurs through both passive diffusion and a saturable carrier-mediated process (Tacnet et al., 1990). Absorption via the saturable carrier-mediated process is important for high intestinal concentrations of zinc. Metallothionenes also play a significant role in absorption for high zinc concentrations (Hempe and Cousins, 1991). Furthermore, they take part in zinc homeostasis and their production is amplified due to increased zinc levels (Richards and Cousins, 1975; Cousins, 1985). Not much is known about the exact role of metallothioneins in zinc absorption, but it is thought to regulate zinc availability by binding it in the intestinal mucosal cells, thus preventing absorption and providing an exit route for excess zinc as these cells are shed and excreted in the feces (Foulkes and McMullen, 1987). It was suggested in a study by Hempe and Cousins in 1992 that as zinc enters the cells of the intestinal mucosa, it is initially associated with CRIP, a saturable cysteine-rich intestinal protein and only a small portion of zinc binds to metallothioneins. If intestinal concentrations of zinc continue to rise, CRIP becomes saturated, and therefore binding of zinc to metallothioneins increases.

After crossing the intestines, zinc then binds to plasma albumin and beta-2-macroglobulin where it is carried to hepatocytes. 30 – 40% of this protein-bound zinc is extracted by liver and then released in to the blood stream (Talcott et al., 2001). Zinc is mainly eliminated through pancreatic secretions and bile into the feces. 70-80% of an ingested dose of zinc is excreted in the feces via the gastrointestinal tract. (Davies and Nightingale, 1975). Approximately 14% of the eliminated zinc is excreted in urine (Wastney et al., 1986) through sweat (Prasad et al., 1963), saliva secretion (Greger and Sickles, 1979), and incorporation into hair (Rivlin, 1983) are other minor routes of zinc elimination. The rate at which zinc is excreted is dependent on both past and current zinc intake (Johnson et al., 1988). Age is also another factor that affects the rate at which zinc is excreted. In 1991 He et al. reported higher fecal excretion of zinc in adult mice following an intraperitoneal dose of ^{65}Zn, as compared to younger mice (weanling, adolescent, or young adult mice).

1.3 Zinc Cytotoxicity

In this study the toxicity of zinc has been directed towards neurons but it has been reported in many studies that zinc is also toxic to others cells in the body. Zinc toxicity may occur due to high oral doses of zinc salts in mammals (> 20 g/day). Inhalation of zinc fumes over a few hours of less than 20 mg zinc salts can be followed by the symptoms of the metal fume fever and can therefore induce toxicity. Patients diagnosed with zinc toxicity are treated by chelating therapy to remove increased zinc from the body. However, mortality is high in cases involving severe zinc intoxication. This might be due to the association of many organs in the zinc-mediated dysfunction:

pancreas, liver, kidney, heart and hematological system. Numerous animal studies have been conducted suggesting that high levels of zinc induce toxicity which may affect different organs. Recently, Dyk et al. investigated histological changes in the liver of Cichlidae fish after exposure to zinc. The livers appeared soft and several histological changes were present which indicated metal toxicity. These histological changes reported included hyalinization, hepatocyte vacuolation, cellular swelling, and congestion of blood vessels (Dyk et al., 2007). In another study low levels of zinc acetate and zinc chloride were applied on the skin of rabbits and mice. Skin irritations were observed on these animals (Gilmour et al., 2006).

Various observations and studies involving human populations who have been exposed to zinc have revealed the evidence of toxicity with increased levels of zinc in their systems. EHC-93, an atmospheric dust sample is known to induce lung cell injury and inflammation (Adamson et al., 1999). In a 3-day study, a solution containing all metals present in EHC-93 and that of a zinc salt alone resulted in an increase in inflammatory cells, protein in lung lavage fluid, and DNA synthesis in lung cells. But only the zinc salts stimulated rapid focal necrosis of type 1 alveolar epithelial cells followed by inflammation and amplification of protein levels in lavage fluid in a 28-day. At 4 weeks, following the injury, epithelial cell proliferation was enhanced and focal fibrosis was observed. When zinc salt was applied at a 10x dose, the pulmonary changes were significantly enhanced. This study shows that the toxicity associated with EHC-93 atmospheric dust is almost certainly due to the level of soluble zinc in this particulate sample. This indicates that enhanced zinc content of atmospheric dust may possibly be

a fundamental factor in determining pulmonary cell reactivity to inhaled particulates (Adamson et al., 1999).

Another study showed that cardiac injury may be induced by pulmonary zinc exposure. Impaired mitochondrial respiration, stimulated cell signaling, altered Ca2+ homeostasis, and increased transcription of sulfotransferases were suggested to be a result of the direct effect of zinc on myocardium following pulmonary exposure (Gilmour et al., 2006).

Also, pulmonary exposure of a rat model to zinc showed cardiac, coagulative, and fibrinolytic alterations. This study demonstrated that cardiovascular blood coagulation impairments are expected following pulmonary zinc exposure and associated pulmonary injury and inflammation (Gilmour et al., 2006).

1.4 Zinc Involvement in Brain Disorders.

Zinc levels and its role in the brain diseases have become an important area of study. Recently, there have been numerous reports on the involvement of zinc in Alzheimer's Disease (AD). It's already known that AD is associated with the abnormal aggregation of beta-amyloid protein (Aß) in the brain and many studies have confirmed that certain metals play a role in the precipitation and cytotoxicity of this protein. Zinc was shown in 1993 to promote aggregation of plaques in AD (Mantyh et al., 1993). More recently, In 2006, a study suggested that Aß complexed with zinc and that this complex was more toxic than Aß by itself (Chen et al., 2006). Normally most of the zinc present in the brain is sequestered in cellular compartments or tightly bound to specific proteins. Zinc is released from presynaptic terminals upon stimulation of zinc-containing

pathways. However, excessive zinc translocation and accumulation from pre- to postsynaptic neurons contributes to the selective nerve cell injury seen in cerebral ischemia, epilepsy, and brain trauma. This increase in intracellular post-synaptic zinc strongly corresponds with neuronal damage, suggesting a role for zinc in cellular injury (Young et al., 2007). Studies have suggested that zinc destroys neurons by inhibiting ATP synthesis at the level of mitochondria. Cytochromes b and c1 complex have been shown to be reversibly inhibited by zinc (Dineley et al., 2003). Cells undergo apoptosis when exposed to lower levels of zinc (< 30 μM). However, necrosis is observed under higher exposures (Kim et al., 1999). Also, at higher zinc concentrations, neurons have the capability to alternatively induce proteins such as metallothioneins that bind zinc, decrease its intracellular level, and therewith provide protection (Ravid et al., 2006). Despite the numerous studies conducted to further investigate zinc toxicity, much about effects of excess zinc on various processes in the body still remains unknown.

1.5 Zinc and Cancer

Zinc had not been listed as a carcinogen but has been suggested to play a role in cancer cells. Numerous studies have investigated the affect of zinc on cancer cells. Concentrations of 150 μM or higher resulted in apoptosis and necrosis in thyroid cancer cell lines (Iitaka et al., 2001). Also, zinc has been shown to induce apoptosis in HEP-2 cancer cell line which was established from human laryngeal carcinoma (Rudolf et al., 2005). The direct application of zinc to prostate cancer cell lines has also shown evidence of apoptosis (Uzzo et al., 2002). An interesting study in 2005 showed that the antibiotic, clioquinol served as a zinc ionophore when applied to cancer cells. The

significant increase in intracellular zinc from the clioquinol reduced cell viability in eight different cancer cell lines. Also in the same study, clioquinol inhibited tumor growth of xenografts over a 6-week period, in an in vivo xenograft mouse model (Ding et al., 2005). These studies imply that inducing high levels of intracellular zinc in malignant cells may have an anti-cancer effect. This approach could used as effective therapy against many tumors.

It is very interesting that reducing zinc levels below normal may also control cancer cells. For example, in both breast and prostate cancer cells, zinc is significantly decreased due to a reduction of zinc transporters which are capable of moving zinc into the cell. Investigations of zinc involvement in breast cancer have just recently emerged with findings showing the presence and function of LIV-1 protein, a zinc transporter (Taylor et al., 2004). Perhaps more importantly, a recent study showed evidence indicating a negative correlation between LIV-1 protein expression and tumor size, grade, and stage (Kasper et at., 2005). More research has been done toward prostate cancer and zinc. The highest levels of zinc are seen in normal human prostate tissue when compared to any other soft tissue in the body. It is already known that prostate epithelial cells normally accumulate zinc and loss of this function turns them malignant due to the mislocation or reduced generation of the zinc transporter proteins, ZIP-1, ZIP-2 and ZIP-3 (Desouki et al., 2007).

1.6 Proposed Research and Contributions

Given the evidence that zinc can have toxic effects on tissue of the central nervous system (CNS), it is essential to quantify both its neurotoxicity and functional

toxicity. The latter term is used here to describe interference with the normal electrophysiological mechanisms of neural tissue without causing cell death. The temporal evolution of these forms of toxicity as a function of zinc concentration is not well documented. Also, the influence of tissue electrical activity on the progression of toxicity and the major cellular entry channels involved are poorly defined and still controversial. To help understand these processes, we have used murine frontal cortex tissue for the formation of spontaneously active networks on optically transparent microelectrode arrays. This approach provides morphological information and multichannel electrophysiological data on action potential patterns in a small nerve cell network and is well suited to answer some of the questions raised above.

Spontaneously active neuronal networks grown on substrate integrated microelectrode arrays (MEAs) in vitro have been used for many studies of pharmacological and toxicological responses to known and unknown compounds (Gross et al., 1995; Gramowski et al., 2000; Morefield et al., 2000; Keefer et al., 2001a; Gross and Pancrazio, 2006; Gross and Gopal, 2006). Although such changes must be considered "cell culture correlate responses" to the altered behavioral or life-threatening changes that occur in animals, these networks function as physiological sensors as they are capable of generating activity changes in the same concentration ranges that alter functions of an intact mammalian nervous system (Xia et al., 2003; Xia and Gross, 2003; Gross and Gopal, 2006). EC_{50} values are in the same range as those published for other preparations and often overlap with those obtained from animal experiments. It is apparent that the major receptor, synaptic, and cellular mechanisms responsible for basic pattern generation in CNS tissues, are represented in neuronal primary cell

cultures. There is now little doubt that such cultures provide histiotypic pharmacological responses (Gross and Gopal, 2006).

This report quantifies temporal electrophysiological and morphological changes in cultured neurons as a function of concentrations of added zinc acetate ranging from 20 μM to 2 mM in normal medium with serum and in serum-free and albumin-free medium. Concentrations below 20 uM added to cultures lacking serum and albumin did not result in any electrophysiological changes. If serum and albumin were present, then concentrations below 175 uM did not cause electrophysiological activity changes to occur. The research shows that temporal electrophysiological and morphological changes in neurons are a function of zinc concentration and that electrophysiological deficits occur before major morphological changes are manifest. As zinc enters the cell and electrical activity deteriorates, specific morphological changes take place. The primary feature is neuronal cell swelling and frequent lysis, implying ion deregulation with increases in cellular osmolarity. To observe these changes, 20% cell swelling was linked to the time and percent activity loss after a specific concentration of zinc was added. All zinc concentrations tested created an excitatory phase before the onset of irreversible activity decline. In order to quantify this excitation phase, the duration and percent increase from reference activity was analyzed. In this report we have confirmed that zinc neurotoxicity is indeed linked to spontaneous activity.

No reports have been found that link the spontaneous electrical activity of neural tissue networks to zinc exposures. Consequently, the evolution of toxicity as reflected in the pharmacologically sensitive network electrical activity is not defined. In addition, the relationship between declining activity and cellular morphological changes is unknown.

Finally, it is possible that major electrophysiological changes can occur at low zinc concentrations in the absence of general neuronal death. This too is presently unknown.

This dissertation addresses these questions using parallel, multiunit recording of spike activity generated by murine networks growing on microelectrode arrays in culture. Such a methodology is shown to be well suited for quantitative investigations of zinc neurotoxicity and cytotoxicity.

CHAPTER 2

MATERIALS AND METHODS

2.1 Microelectrode Array Fabrication and Cell Culture

Microelectrode arrays (MEA) were fabricated in-house and prepared according to methods described previously (Gross, 1994; Gross et al., 1985; Gross and Kowalski, 1991). Briefly, indium–tin oxide (ITO)-sputtered glass plates were photoetched, spin-insulated with methyltrimethoxysilane, cured, deinsulated at the electrode tips with laser shots, and electrolytically gold-plated to adjust the interface impedance to 1 MΩ at 1 K Hz (Gross et al., 1985). The MEA insulation material is hydrophobic, and butane flaming was used to activate the surface and generate a hydrophilic adhesion island (3 mm in diameter) centered on the MEA (Lucas et al., 1986; Gross and Kowalski, 1991).

Frontal cortex tissue was dissociated from 15- to 16-day-old BALB/c/Icr murine embryos and cultured according to the methods of Ransom et al., (1977) with minor modification that included the use of DNAse during tissue dissociation. The cells were seeded on the MEAs as 0.1 ml droplets with subsequent addition of 2 ml of medium confined to a 4-cm^2 area by a silicone gasket. The care and use of, as well as all procedures involving, animals in the study were approved by the institutional animal care and use committee of the University of North Texas and are in accordance with the guidelines of the Institutional Care and Use Committee of the National Institute on Drug Abuse, National Institutes of Health, and the Guide for the Care and Use of Laboratory Animals (Institute of Laboratory Animal Resources, Commission on Life Sciences, National Research Council, 1996).

The dissociated cells were incubated in Dulbecco's modified minimal essential medium (DMEM) supplemented with 5% horse serum, in a 90% air and 10% CO_2 atmosphere. No antibiotics/anti-mitotics were used. Fig. 1 shows a 13-week old culture on a 64-electrode MEA together with examples of phase contrast images of living neurons on such arrays.

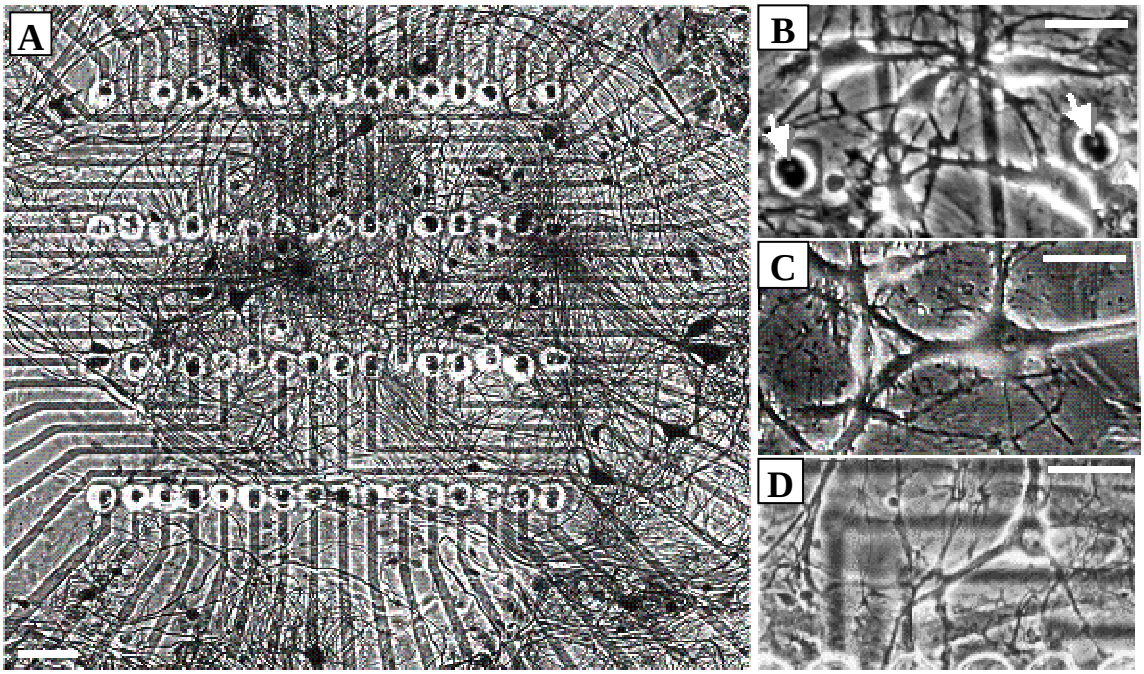

Figure 1. Example of neuronal circuits on microelectrode arrays. Transparent indium-tin oxide (ITO) conductors allow extensive optical access to the network morphology. (A) Neuronal network derived from murine spinal cord tissue (92 days *in vitro*), grown on the recording matrix of a 64-electrode array plate (Bodian stained). (B-D) Living neurons on MEAs. Recording sites (Gold-plated, exposed ITO conductors are shown by arrows in (B)). The ITO conductors are 8 μm wide and 1200Å thick. bars = 50 μm. (CNNS Archives)

2.2 Pharmacological Manipulations & Life Support

Zinc acetate, tetrodotoxin (TTX), lidocaine, verapamil, omega-conotoxin MVIIA (SNX-111), magnesium chloride ($MgCl_2$), NBQX (2,3-dihydroxy-6-nitro-7-sulfamoyl-benzo[f]quinoxaline-2,3-dione), and bicuculline were all obtained from Sigma Aldrich (Sigma Aldrich, inc., St. Louis, MO, www.sigmaaldrich.com) . Table 1 includes a list of these compounds along with the concentrations added. All compounds were diluted in water since all were water soluble. Also all the compounds except for zinc acetate were completely reversible and nontoxic when added to cultures (see appendix).

Table1. List of compounds used.

Compound	Concentration Range
Zinc Acetate	20 μM -2 mM
TTX	200 nM
Lidocaine	250 μM
Verapamil	80 μM
SNX-111	75 μM
$MgCl_2$	10 mM
Bicuculline	40 μM
NBQX	80 μM

To obtain relatively even distributions, the drugs were micropipetted into the culture medium near the edge of the circular chamber at four cardinal positions (separated by 90°). Thorough mixing was achieved by gentle back and forth movement of the medium (normally about 50% per cycle 4-5 cycles) via syringe attached to one of the Luer ports.

To remove the test drug, syringes were used to extract the medium through the same Luer connections at the edge of the recording chamber. These connections lead through 0.8 mm conduits in the stainless steel to an orifice inside the 'O' ring situated approximately 100-200 μm above the surface of the MEA inside the 'O' ring (Gross, 1994).

Microelectrode arrays were placed into recording chambers (Gross, 1994, Gross and Schwalm, 1994) and sustained at 37°C on a microscope stage. The pH was maintained at 7.4 with a continuous stream of humidified 10% CO_2 and 90% air at 5–10 mL/min into a special cap fitted with a heated ITO window to prevent condensation. The syringe pump, Harvard Apparatus® Pump II (Harvard Apparatus, inc., Holliston, Massachusetts, www.harvardapparatus.com) compensated for water evaporation (30 to 60 μl/hr depending on set-up). During experiments, pH and osmolarity were tested at intervals of 2-3 hours. Despite the limited medium volume in the chamber (2 mL), the pH could be tested by extracting 100 μL volumes with a pipette and measuring pH in the pipette tip. This could be accomplished with an Accumet flexible glass pH microelectrode that has such a small sensor diameter as to allow entry into the pipette tip and a friction-fit stabilization of the pipette tip. In this manner temperature equilibrium and stability could be achieved for measuring. After pH measurements, 10 μL of the medium were extracted for osmolarity determination with a Wescore 5500 vapor pressure osmometer. This special protocol allowed frequent measurements without exhausting the medium volume in the chamber and compromising sterility. pH values between 7.35 and 7.45 +/- .05 were accepted as they had little influence on overall activity. Osmolarities were not allowed to fluctuate more than 10% from a reference of

320 mOsmoles. Between 290 and 340 mOsmoles, neurons osmoregulate without measurable activity variations if the changes are slow (10 mOsm per minute). Rapid medium replacements require osmolarity matching to within 10 mOsm. Water additions are tolerated generally up to 5% of the total volume.

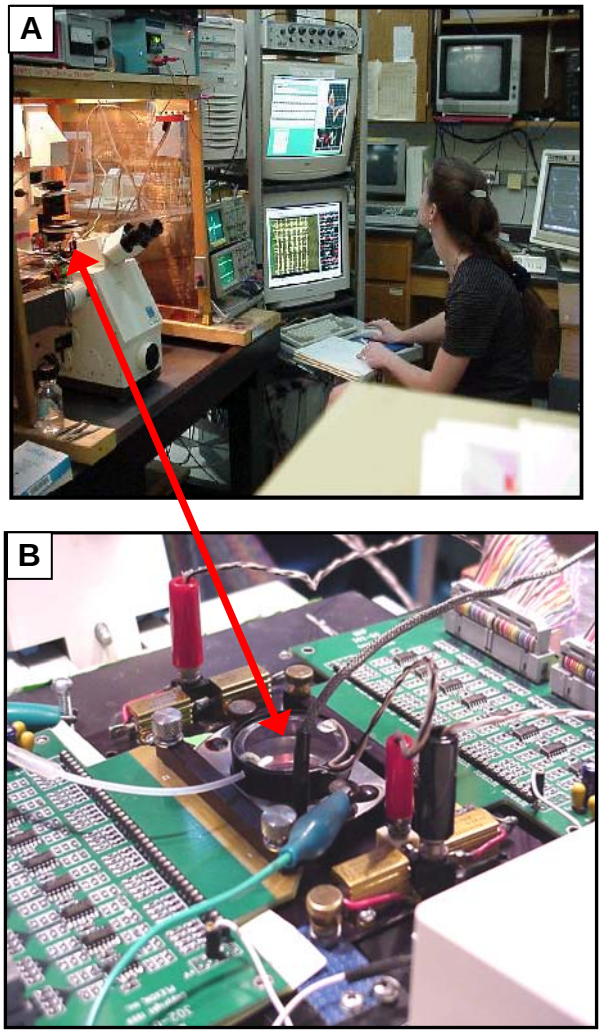

Figure 2. Experimental Workstation. (A) Faraday cage with inverted microscope and culture life support equipment. Oscilloscopes and two monitoring screens display data digitized by Plexon multichannel data amplification and processing system. (B) Recording chamber on microscope stage with plexon preamplifiers attached. A cap with heated window covers the medium bath and maintains the 10% CO_2 atmosphere while allowing continual microscope observations. (CNNS Archives)

2.3 Recording Environment and Data Analysis

After assembly, neuronal activities were monitored on oscilloscopes in real time to provide spike information. Recording was performed with a commercially available, computer-controlled, 64-channel data acquisitions and processing system (Plexon Inc., Dallas, TX, www.plexoninc.com). Preamplifiers were placed on the microscope stage to both sides of the recording chamber and connected to the MEA by means of zebra strips (Fujipoly America Corporation, Carteret, NJ, www.fujipoly.com). Total system gain was set to 10,000. The amplifier ground was connected to the stainless steel chamber confining the culture medium. An important feature of network activity is the organization of action potentials (spikes) into high-frequency clusters (bursts). Burst patterns represent a simplified level of activity and often reveal the major modes of network behavior (Gross, 1994; Keefer et al., 2001c). Integration was used to simplify the identification and quantification of bursts. All analyses were done with binned data (bin size of 60 s). Single-unit activity was averaged across the network to yield mean spike rate, burst rate, burst duration, and integrated burst amplitude per minute. In order to avoid excessive network responses to medium changes required for the washout of substances, the native medium was exchanged for the wash medium (fresh DMEM stock) at the beginning of the experiment, and the cultures were allowed to stabilize before any drugs were added (termed reference activity). The percent change in activity for each variable at each zinc or drug concentration was always calculated relative to this 20- to 60-min reference spontaneous activity. To follow the changes in network activity with time, spike rates and burst rates, averaged across all active units selected per minute, were plotted as a sequence of "minute means" in real time.

Bursts were identified operationally by digital RC integration with rise time constants of approximately 100 ms. Two thresholds (Fig. 2) were used: a lower threshold to determine the start and stop times for the burst and a higher threshold to confirm that the integrated profile was above the noise level. A gap rule of 100 ms devoid of spikes was used to separate burst events into two bursts (Morefield et al., 2000). T1 and T2 were set by inspection during off line data analysis with the intent to capture major bursts and ignore spike clusters of 2 to 4 spikes. Raster displays showing spiking and bursting were viewed with the Neuroexplorer® program (NEX Technologies, Littleton, MA, www.neuroexplorer.com) and thresholds were set to mimic the burst count in initial segments of the native activity. This operational definition allowed quantitative comparisons of burst patterns within the same culture if thresholds were not changed.

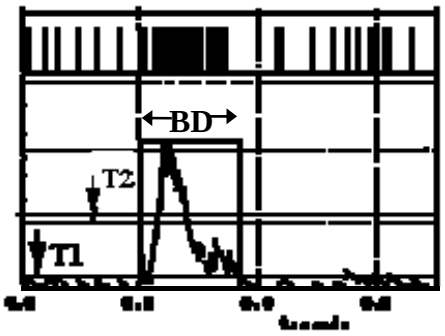

Figure 3. Burst detection method. Time stamp sequence of a discriminated unit and mathematically simulated RC integration. The two thresholds (T1 & T2) identify sufficiently large bursts with accurate start and stop times. BD: Burst Duration. (CNNS Archives).

2.4 Cell Swelling Analysis

After the application of zinc, neurons showed extensive swelling and consequent lysing. Cells in culture were observed with a microscope at the time of recording. An area of the culture including 8 or more neurons was chosen and analyzed. Consecutive pictures were taken before and after the application of zinc using the software, Frame Grabber® (Integral Technologies, inc., Indianapolis, IN, www. integraltech.com) Cell swelling analysis was done for four different concentrations of zinc (50, 200, 500, 1000 μM) added to cultures. Pictures of the area initially selected for analysis were taken every 1-2 minutes due to the concentration of zinc added until the cells were completely lysed. Evaluation and analysis of somal swelling was done using the software, ImageJ® (National Institute of Health). The soma were observed and traced manually 3 times to obtain an area for each picture taken. Because all data were expressed in percent change, no calibration was attempted and numbers are in arbitrary units. If the coefficient of variation for the three values obtained from the tracings was below 5% then the average from those three values was recorded and used for analysis. An example of the tracings is shown in figure 4 and the values obtained for areas, the average, and coefficient of variation are shown in Table 2.

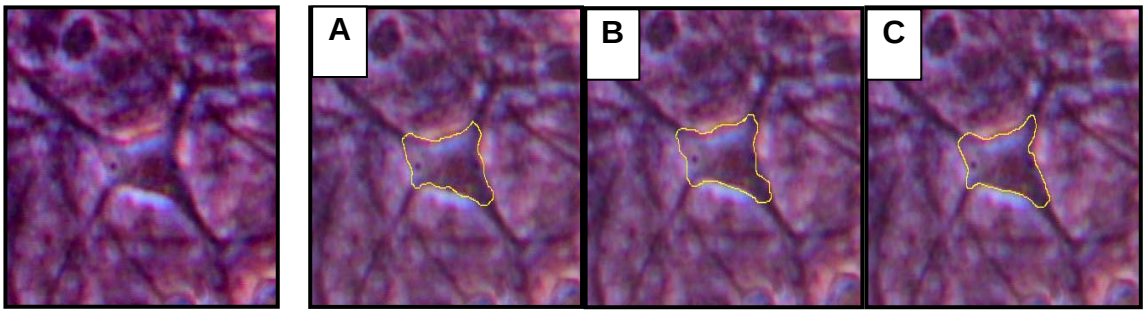

Figure 4. Manual tracing of soma to obtain area (in arbitrary units). Line around the perimeter of the soma were drawn three times (A,B,C).

Table 2. Sample values obtained from the manual tracings shown in Fig 3. The average (avg.) of the three values of A, B, and C is given along with the standard deviation (SD) and coefficient of variation (CV).

	Area
A	4125
B	4324
C	4254
avg.	4234.3
SD	100.9
CV	2.36%

2.5 Statistics

Where appropriate, data are presented as mean +/- standard deviations and (n) number of experiments performed. Statistical significance was determined by t-tests with $P<0.05$ considered as significant. 95% confidence limits for Fig. 13 were calculated using Microsoft® Excel software (procedure explained in Appendix C).

When determining the significance between a chosen set of values and time to 50% and 90% activity loss at certain concentrations, two types of t-tests where conducted using the one-sample and unpaired from Graphpad® Software (Graphpad Software, inc., San Diego, CA, www.graphpad.com). Individual values from experiments where compared to the theoretical 50% & 90% activity loss which is derived from equation 1 and experimental 50% & 90% activity loss which is the calculated mean of experimental values. Both t-tests were used to determine statistical significance between the time to 20% cell swelling and time to 50% activity loss at different zinc concentrations (Fig 14). Also, t-test were used to determine statistical significance between time to 50% and 90% activity loss in cultures with 500 μM zinc with or without NBQX pretreatment (Fig. 20) or with or without SNX-111 pretreatment (Fig. 23).

CHAPTER 3

RESULTS

3.1 Basic Network Responses to Zinc

3.1.1 Responses to High Concentrations

The typical network activity response to high concentrations of zinc is shown in the spike and burst rate plot of Fig. 5A. The plot depicts the temporal evolution of spike and burst activity averaged across all discriminated, digitized units in one-minute bins. After a 38 min period of stable spike and burst activity, the addition of 200 μM zinc acetate to the bath medium resulted in a rapid (2 min delay) 120% increase in spike activity and a 140% increase in burst rate lasting approximately 50 min. Note that spike and burst data follow each other closely. Thereafter, activity declined until it reached catastrophic network failure at 145 min. Network bursting ceased at approximately 130 min. This activity loss was irreversible, as demonstrated by the lack of response to two complete medium replacements. Concomitant to the activity loss, neurons undergo time-dependent morphological changes. Neuronal somata show clear swelling with development of cytoplasmic granularity. The nucleus showed no overt effects until after major necrotic changes had occurred. The flat glia carpet showed condensation of cytoplasmic components and apparent swelling of some cells (compare panels B3 & 4 with B1). The neuronal cellular destruction is global as no nerve cells were spared.

The raster display (spike time stamp pattern) from the 49 discriminated units plotted in Fig. 5 is shown in Fig. 6A for four time periods**:** native activity (at 20 min), the excitatory phase (at 60 min), and activity decay (at 110 & 120 min). This display shows changes in the activity pattern that are, however, difficult to quantify. A simple

quantification is shown in Figs 6B and C were the number of active units, the number of bursting units, the mean burst duration, and the burst period are plotted in one minute bins. To eliminate contributions from electronic noise, active neurons were defined as those units having more than 5 spikes per minute. Bursting neurons had to have one identified burst per minute. The burst duration is defined in the methods section (Fig. 3). This variable represents the average across all units per minute. An abrupt decrease in active and bursting neurons starts at 110 min with the number of bursting neurons dropping off more sharply. At that time the mean burst duration shows a substantial increase until it undergoes a sharp drop at a 145 min. It is interesting to note that, at 135 min, the active neurons have decreased by 90% whereas the burst duration of the remaining 10% increased by 280%. The network dies by losing units and not by progressive reduction in burst duration. Fig. 6B shows a sharp drop in the mean burst period upon application of zinc, revealing the main reason for the spike rate increases shown in Fig. 5. Zinc addition reduced burst periods resulting in higher burst rates and greater network spike production. The minute to minute fluctuations of the mean burst periods are reduced substantially after the application of zinc. Between 0 and 40 min the mean burst period is 3.29 sec ± 0.33 SD. After addition of zinc (45 and 90 min), this variability is reduced to 1.37 sec ± 0.09 SD. The coefficients of variation change from 10.2 to 6.9, reflecting a greater regularity of burst periods after zinc application. This can be verified qualitatively by inspection of the raster display panels of Fig. 6A. Zinc acetate was applied in 40 μL of a 10 mM stock solution to give the final concentration of 200 μM in the 2 mL constant medium bath. This constitutes a 2% change in medium volume which does not generate osmolarity or pH responses.

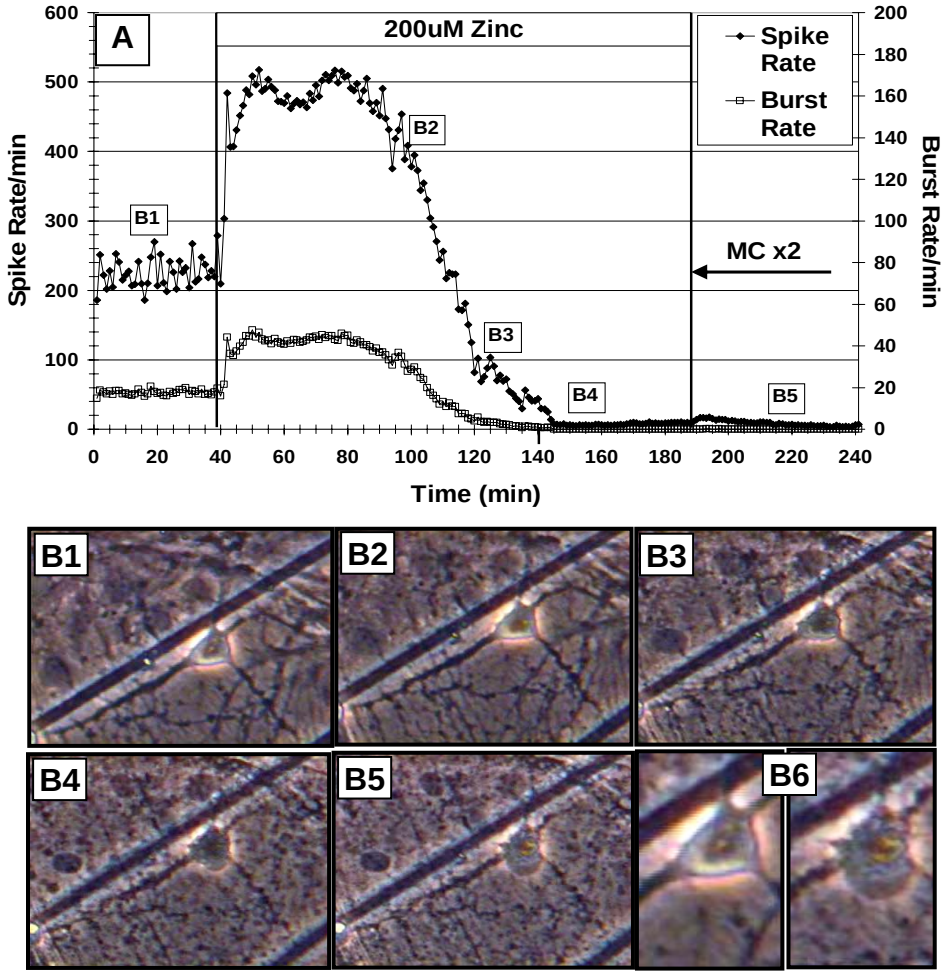

Figure 5. (A) Common network response to high concentrations of zinc. Each data point represents the average spike (left ordinate) and burst (right ordinate) rate in 1 min bins for all discriminated units (n=49). Addition of 200 μM zinc at 38 min results in an immediate excitatory period lasting 70 min followed by activity decay for about 30 min and complete, irreversible activity loss. (B1-B6) Consecutive pictures of the same neuron taken at the intervals shown in A. At 220 min (B5 and B6, right panel), the neuron is swollen and necrotic in appearance. B6 represents enlarged views of B1and B5. Diagonal electrode conductor width is 10 μm.

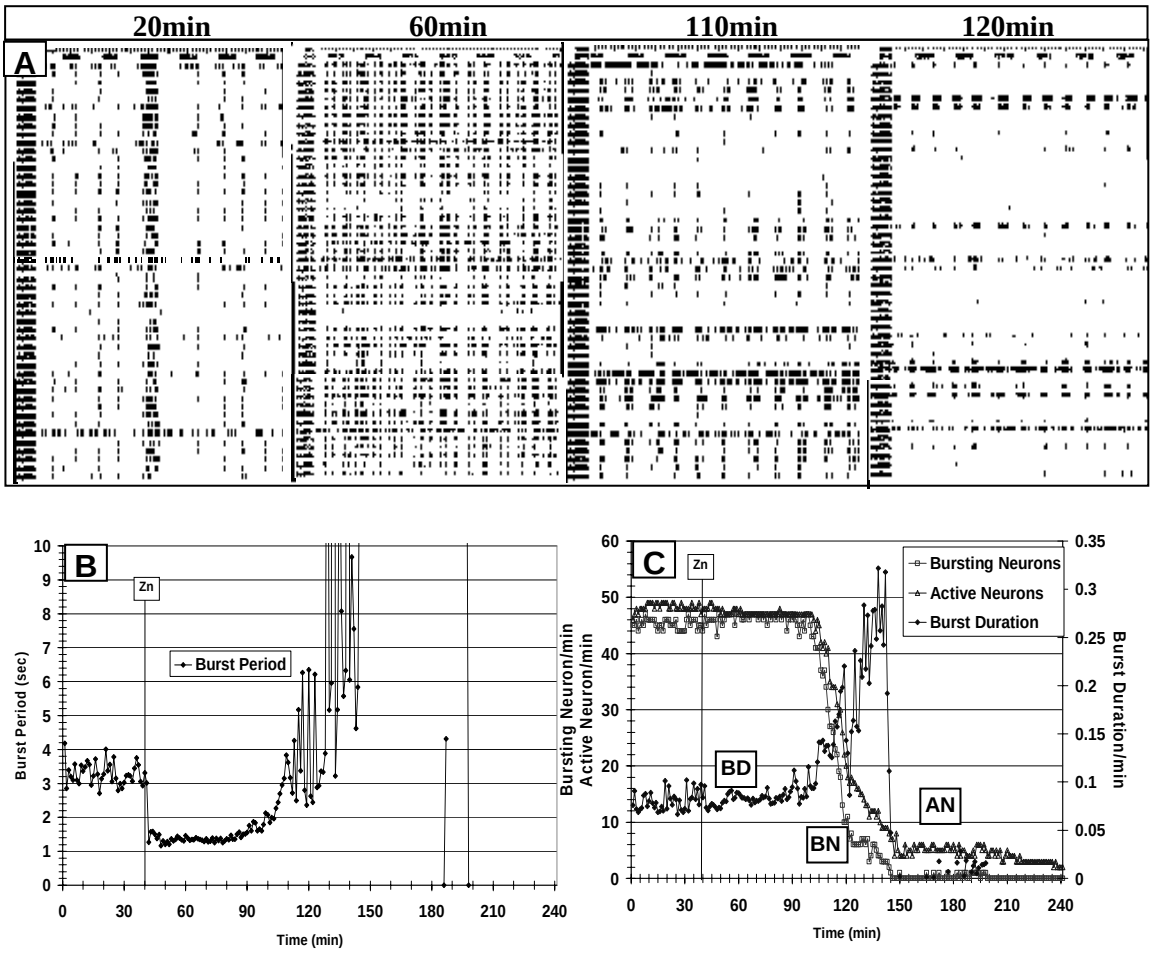

Figure 6. (A) Raster plot of activity over time for four experimental episodes at 20, 60, 110, and 120 min shown in Fig. 3. The excitatory phase, activity decay, and more subtle changes in burst patterns can be observed. Each row represents a discriminated unit. (B.) Temporal evolution of burst period showing a sharp reduction at the moment of zinc application. (C) Temporal changes in active and bursting neurons and in burst duration as a function of time. The application of zinc is shown at 40 min. Data in B and C are presented as global averages per minute. BD: burst duration; BN: bursting neurons; AN: active neurons.

Differences in the responses of individual units are best demonstrated by individual spike rate plots as shown in Figure 7. Here, a remarkable diversity among units can be seen. Whereas all units succumb to zinc toxicity, the respective activities do not stop at the same time and especially the excitatory phase shows substantial variability.

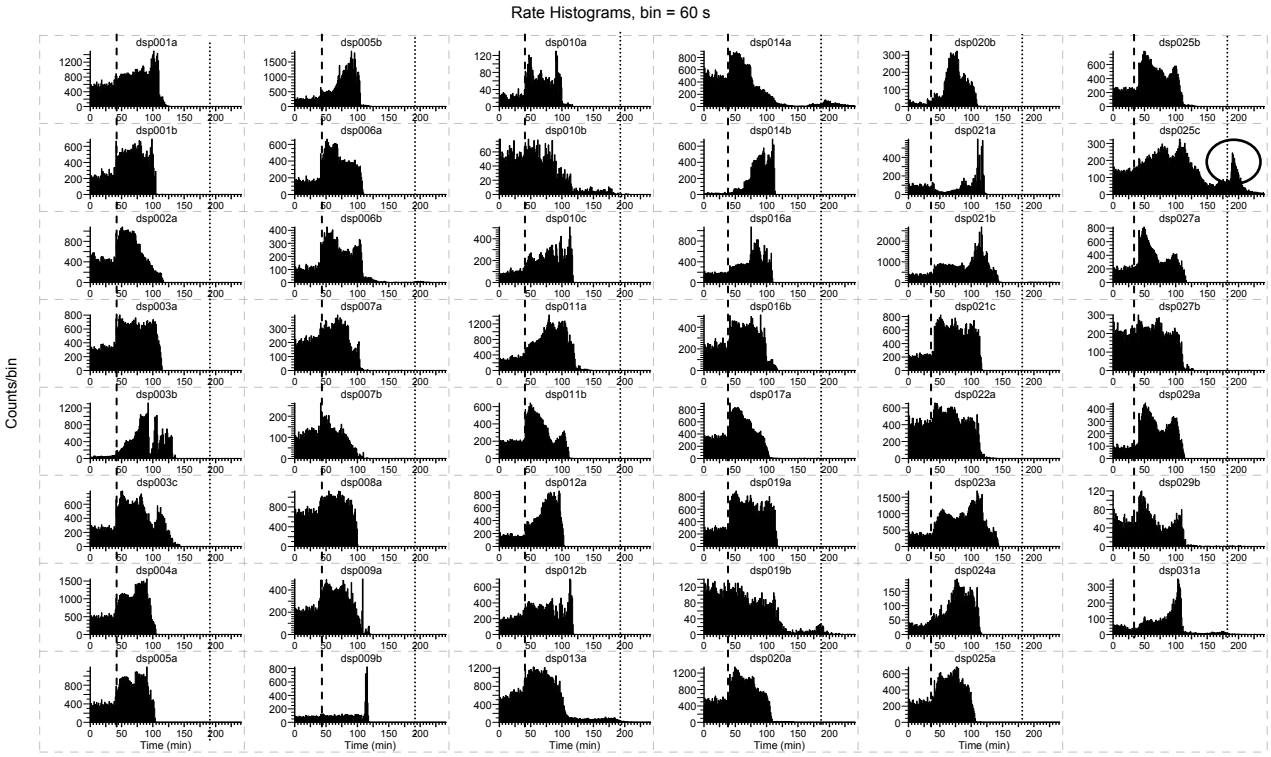

Figure 7. Individual spike rate plots from discriminated units used to generate Fig. 5 are plotted in one-minute bins. Vertical dashed line: application of 200 μM zinc acetate; vertical dotted line: full medium change. Individual profiles show response differences although all of them respond to zinc with activity termination. Rapid excitatory response to zinc is shown by 90% of the population and 83% of the units lost all activity at 125 minutes. Only one unit (circle) displayed a response to the medium change before dying.

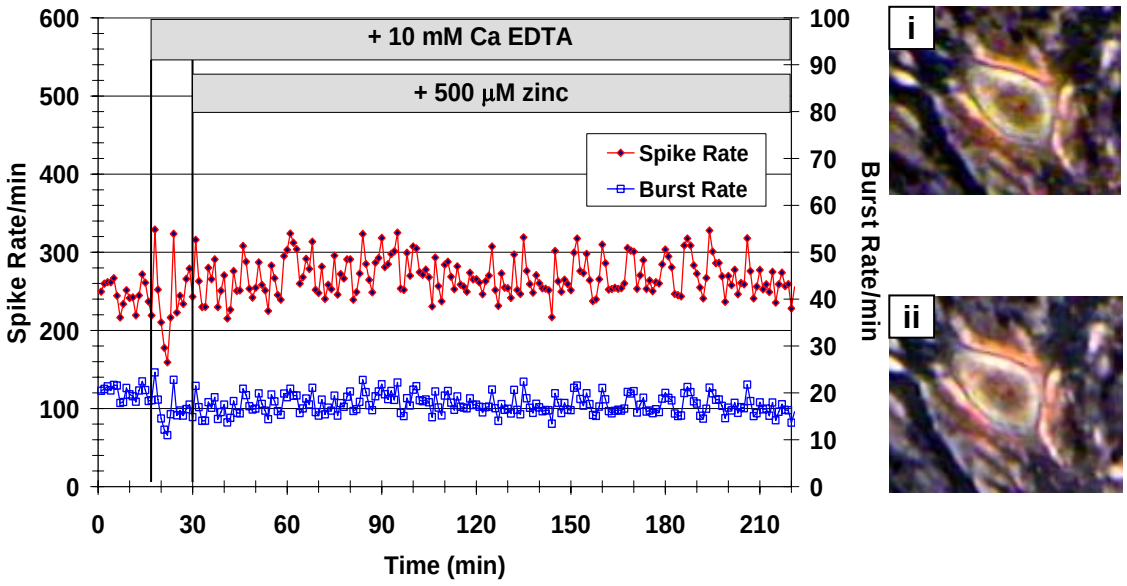

Figure 8. Pretreatment with zinc chelator, Ca EDTA. The addition of Ca EDTA prior to 500 μM zinc application prevented any major changes in electrophysiological activity and cell death. Image of a neuron in culture is shown before zinc application at 5 min (i) and at 220 min (ii).

The addition of zinc specific chelator, Ca EDTA has been known to prevent zinc neurotoxicity and hence protect neurons from contact with toxic amounts of zinc either released presynaptically or added in vivo or in vitro (Frederickson et al., 2002). In order to show that the changes observed in electrophysiological activity, neurotoxicity, and consequent cell death subsequent to zinc additions were actually specific to the actions of zinc, 10 mM Ca EDTA was applied to the culture medium prior to 500 μM zinc addition (Fig 8). Electrophysiological activity remained the same and cell death did not result.

3.1.2 Network Response to Low Concentrations of Zinc.

Zinc concentrations below 20 μM added to cultures did not result in an excitation phase nor did they cause loss of any activity when evaluated for up to 24 hours. Figure 9 compares the change in spike rate activity of cultures responding to 15 and 20 μM zinc. The addition of 15 μM did not cause any changes in network activity, but 20 μM resulted in activity loss and consequent cell death. This suggests that cells in FC culture have the capability to buffer zinc concentrations below 20 μM and concentrations above 20 μM exceed this buffering capacity. To further investigate this buffering capacity, 200 μM zinc was added in 10 μM increments with 20 to 30 min between applications (1-20) as shown in Figure 10. The first application of zinc did not result in any network activity changes, but subsequent ones caused sudden increases followed by stable activity. When stability was established, the next 10 μM dose of zinc was applied until the final concentration of zinc totaled to 200 μM (20^{th} application). Activity decay continued in the next 5 hours until no network spiking was observed and major global cell death occurred. This experiment shows a remarkable cellular adjustment in response to small incremental increases in zinc concentrations. Presumably, this reflects the upregulation of metallothionenes and a consequent stronger buffering (see discussion).

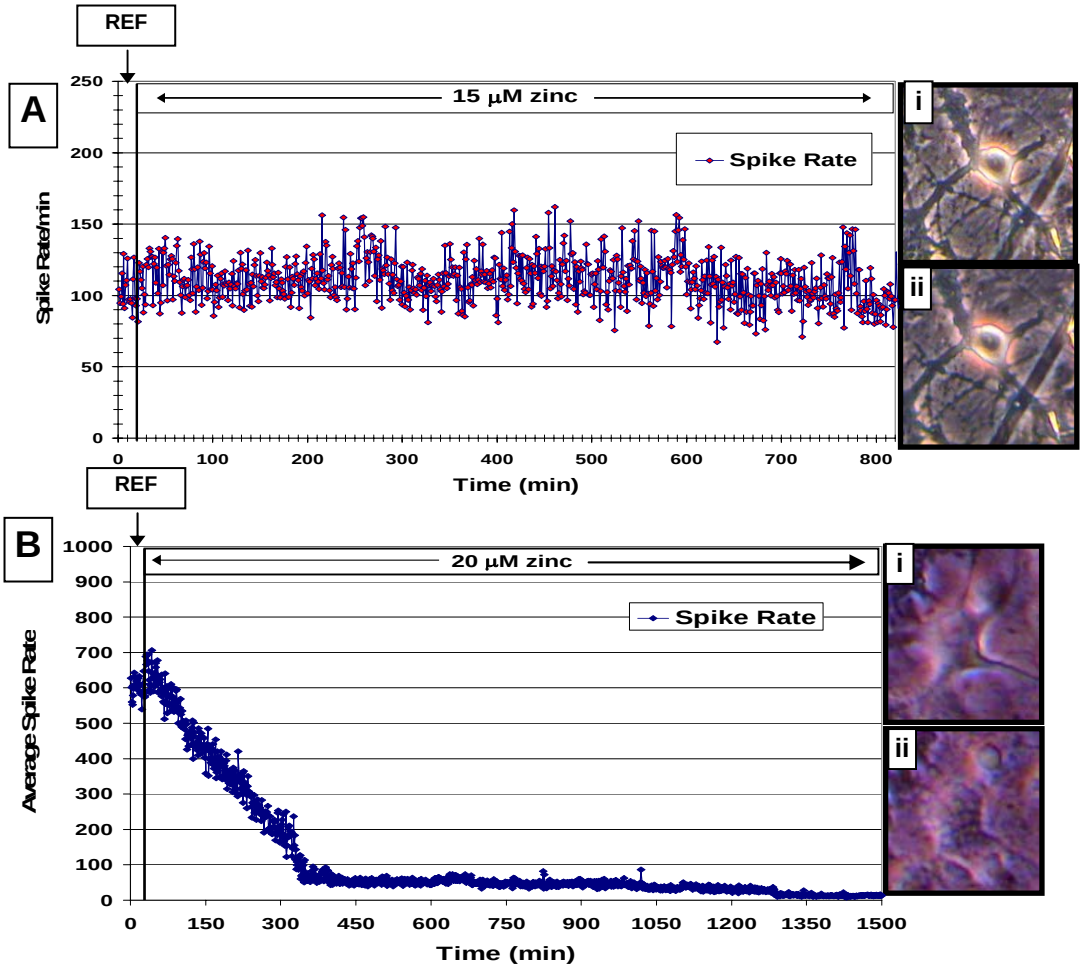

Figure 9. Response to 15 µM (A) (n=2) and 20 µM (B) (n=2) zinc. (i) Neuron at reference activity (REF). (Aii) Neuron at 800 min. (Bii) Neuron at 1500 min. (Cii) Neuron at 700 min.

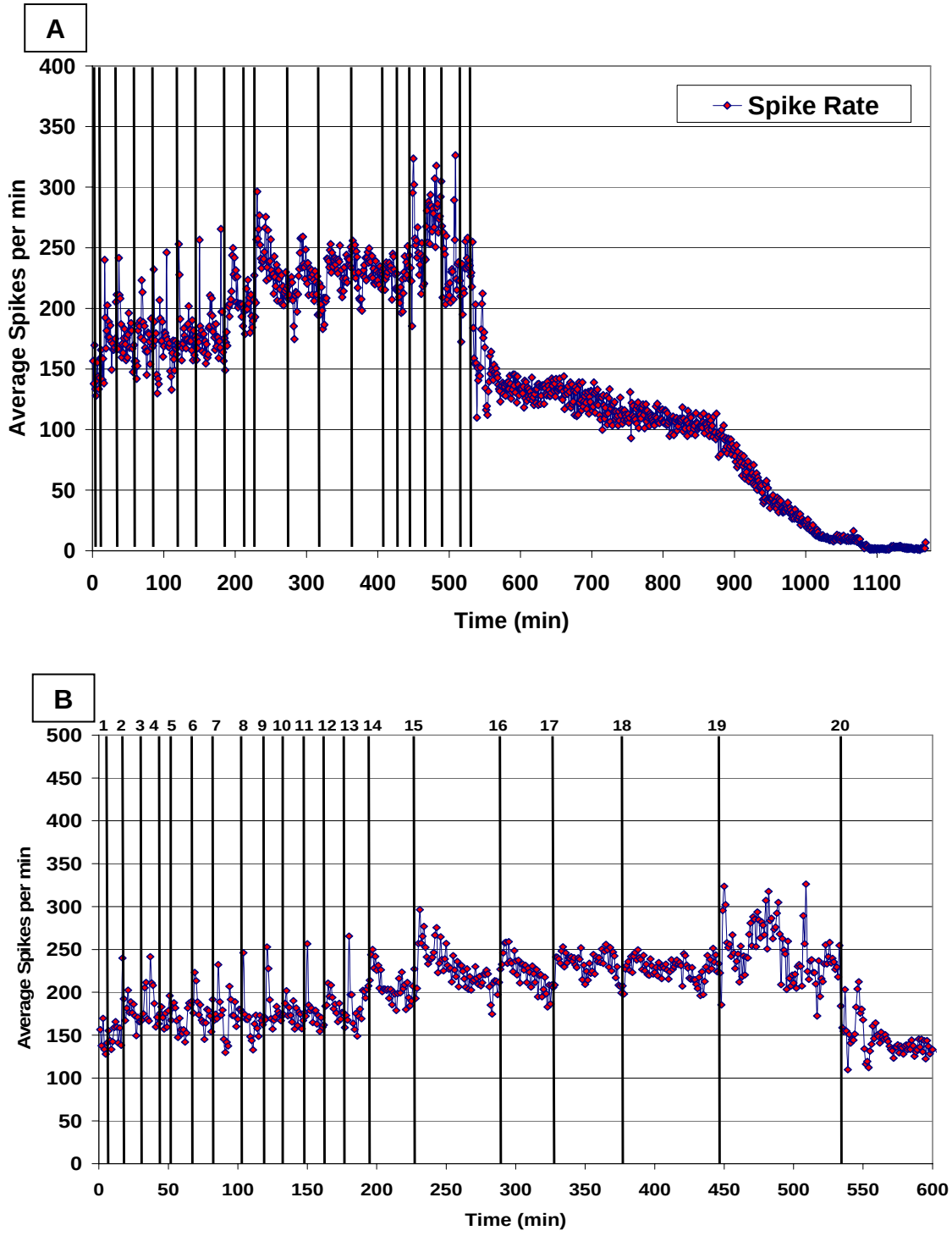

Figure 10. Network accommodation to incremental additions of low concentrations of zinc. 200 μM zinc is added to the culture in 10 μM increments (line). After the last application there is continuous decay of spike rate activity until the culture lost all activity at 1080 min (A). The expansion of A is shown in B.

3.2 Zinc-Induced Excitation

Network excitation immediately following zinc application was seen at all concentrations used above 20 μM. Such excitatory phases are depicted in Figs. 5A, 12A, 15B, and 17A. Although the zinc-dependent subsequent decay of activity is highly consistent, the excitation profiles are quantitatively more variable. This is summarized in Fig. 11 where the maximum percent spike activity increases ranged from 10% to 140%. Profiles are biphasic and ranged from 5 to 60 min with a maximum at 50 μM zinc followed by marked decrease at higher zinc concentrations. The decay of the duration is caused by the rapid spike inactivation and cell destruction at higher zinc acetate additions, which overwhelms the excitation effect.

An interesting observation is the absence of excitation under the influence of the GABA antagonists bicuculline or picrotoxin. Fig. 12 shows results from four experiments where the same concentration of zinc acetate was applied to a network in normal (serum free) medium (12A) and to networks in the presence of bicuculline or picrotoxin. Figs. 12B and D demonstrate the absence of this excitation in the presence of 40 μM bicuculline and 1 mM picrotoxin, respectively. The GABA antagonists need to be applied close to their saturation point to prevent the excitation. A concentration of 200 μM picrotoxin was not sufficient to block the transient excitation that followed zinc application (12C). A total of four bicuculline and two picrotoxin experiments at 40 μM and 1 μM, respectively, have shown a complete suppression of the zinc excitation phase.

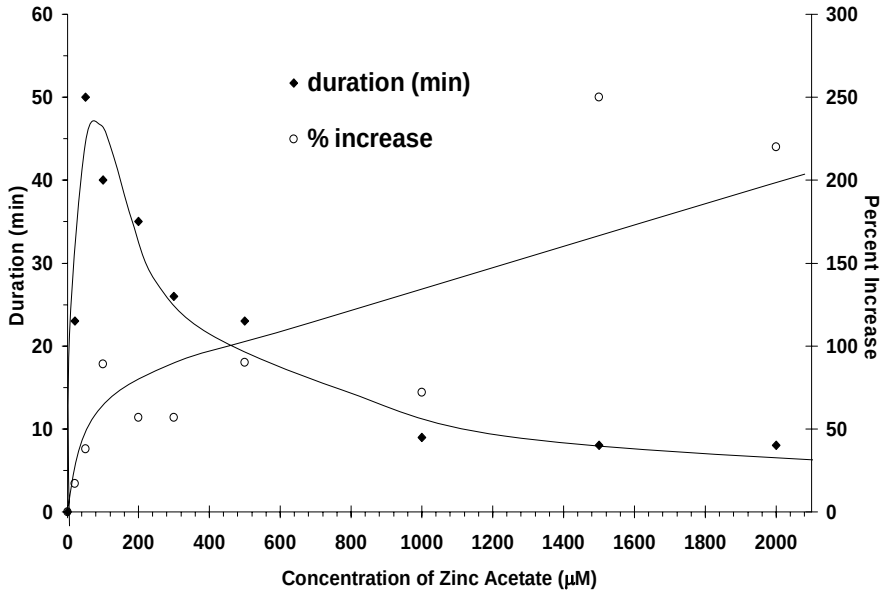

Figure 11. Excitation phase duration (in minutes, left ordinate) and maximum percent increase (from baseline, right ordinate) as a function of zinc concentrations. (n=19 cultures). Values plotted are mean values from 2 to 5 data points. Curve fit was done by inspection.

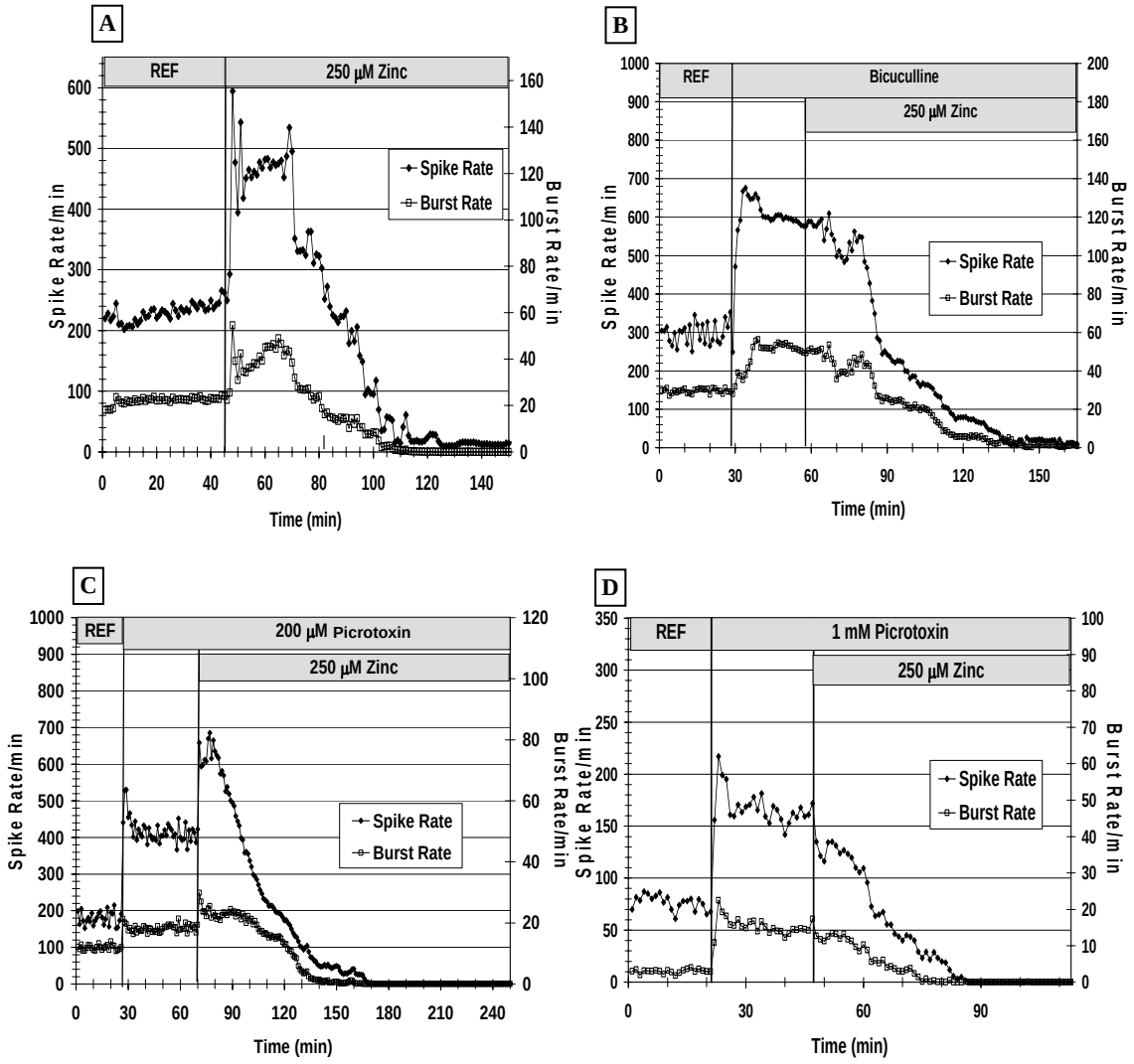

Figure 12. Absence of excitation phase in cultures treated with bicuculline or picrotoxin. (A) 40 min excitation phase peaking at 175% of its native activity induced by 250 µM zinc. (B) Lack of prominent excitation phase when the culture was exposed to 40 µM bicuculline 25 min before zinc was added. (n=3) (C) A network excited by 200 µM picrotoxin (at 28 min) still shows a zinc excitation phase, indicating that $GABA_A$ antagonists need to be near saturation concentrations to prevent zinc excitation (n=3). (D) The excitation phase is absent in cultures under 1 mM picrotoxin (n=3).

3.3 Quantification of Zinc-Induced Temporal Activity Decay

As shown in Figs 5A , 12A, 15B, and 17A network responses are biphasic and consist of an excitatory phase followed by activity loss. The response can be quantified in terms of the time required to reach a certain percentage activity loss. For convenience, we have selected the 50% and 90% mean activity decrease levels and plotted them as a function of zinc concentrations. A linear plot follows a power function that reveals a rapid (10-20 min) activity loss at 2 mM applied zinc acetate and a sharp rise in time at less than 50 μM (shown in Appendix). Between the concentrations of 20 and 2000 μM, the data linearizes well in double log plots (Fig. 13), providing a quantitative measurement of activity loss at applied zinc concentrations. Zinc concentrations including and below 20 μM did not have an effect on the network activity for observation periods up to 30 hours (Fig. 9A).

Experiments were conducted in serum- and albumin-free medium (lower two functions in Fig. 13) as well as in medium containing serum. The sensitivity of network responses is clearly greater in the absence of serum. In medium containing 5% serum, zinc concentrations below 175 μM did not affect the cultures, revealing protection. The linear regressions of time to 50% and 90% activity decay as a function of zinc acetate applied in micromolar concentrations to networks in serum and albumin-free medium are shown in equation 1 and 2. The linear regressions of time to 50% activity loss in those containing serum in the medium is shown in equation 3.

$t = 1841C^{-0.71}$ (1) 50% activity decay, serum and albumin-free

$t = 2902C^{-0.72}$ (2) 90% activity decay, serum and albumin-free

$t = 5601C^{-0.66}$ (3) 50% activity decay, in serum

where C is expressed in micromoles/L and t in minutes. Equation (1 and 2) are defined above concentrations of 20 μM, equation (3) above 175 μM. 95% confidence limits for equation 1 and 2 are included in the Appendix C.

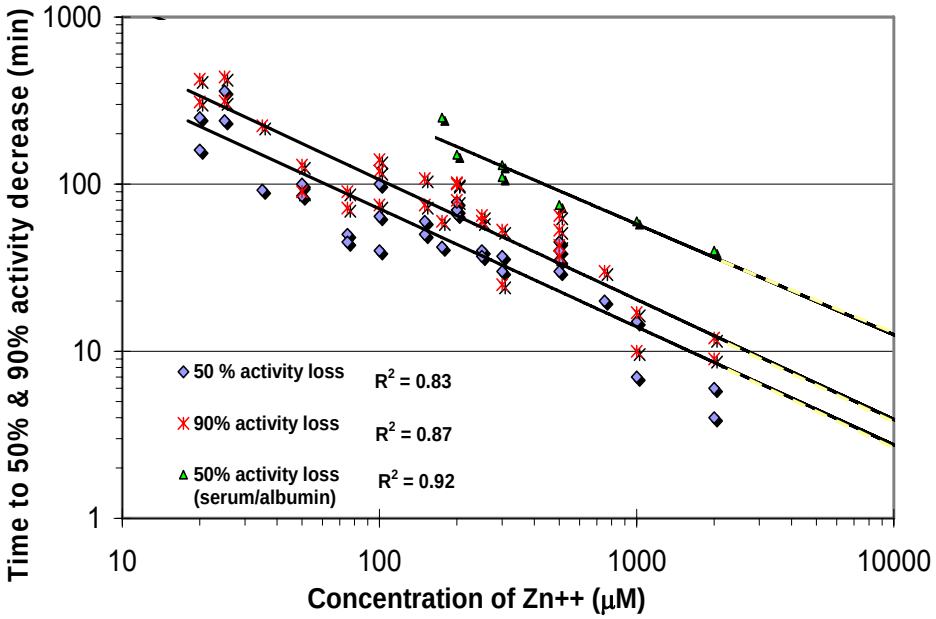

Figure 13. Double log linear regressions for 50% and 90% activity decay in albumin-free and serum-free medium (n = 29). A 50% activity loss function is also shown for experiments in medium containing 5% serum (solid triangles, n = 7). Confidence Limits are shown in Appendix C.

3.4 Relationship between Electrical Activity Deterioration and Specific Morphological Changes

As zinc enters the cell and electrical activity deteriorates, specific morphological changes take place. One of the most prominent morphological features is cell swelling. This change is observed following zinc application at all concentrations which result in cell death (Fig. 15C). To observe these changes, the time it took for neurons in culture to reach 20% cell swelling was compared to the time to 50% activity loss after zinc applications of 50, 200, 500, and 1000 μM (Fig. 14). Statistical significance was not detected between time to 20% cell swelling and time to 50% activity loss for each zinc concentration applied to the culture (t-test, $p<0.05$) therefore suggesting that 20 % cell swelling and 50% network activity loss are closely coupled. There is, however a trend for the 20% cell swelling to occur after the 50% activity loss indicating that 20% swelling may be more accurately coupled to 55-60% activity loss. Neurons evaluated for 20% swelling were of different sizes. Areas (arbitrary values) of soma from cultures treated with 500 μM zinc are shown in Figure 15A (#1-8). Network activity of the neurons selected for evaluation from Figure 15A is presented in Figure 15B. The time when 20% cell swelling occurs for neurons #1-8 is superimposed at relative points during the network response to 500 μM zinc (Fig 15B). The initial soma area did not show a relationship with changes in the rate of network activity loss nor lysing.

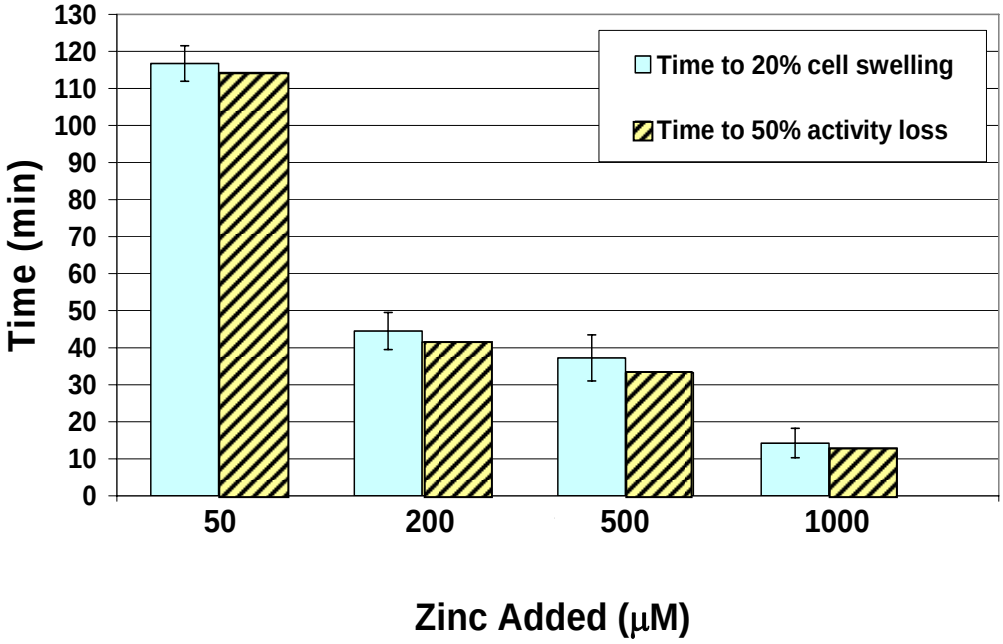

Figure 14. Analysis of cell swelling and activity loss. Comparison between the times it takes for a neuron to swell 20% and 50% network activity loss is shown for each concentration of zinc added to the culture. Values for time to 50% activity loss are derived from equation 1. Statistical significance was not found at each concentration. (Standard deviations are shown with bars for values indicating time to 20% cell swelling. One sample t-test, $p<0.05$).

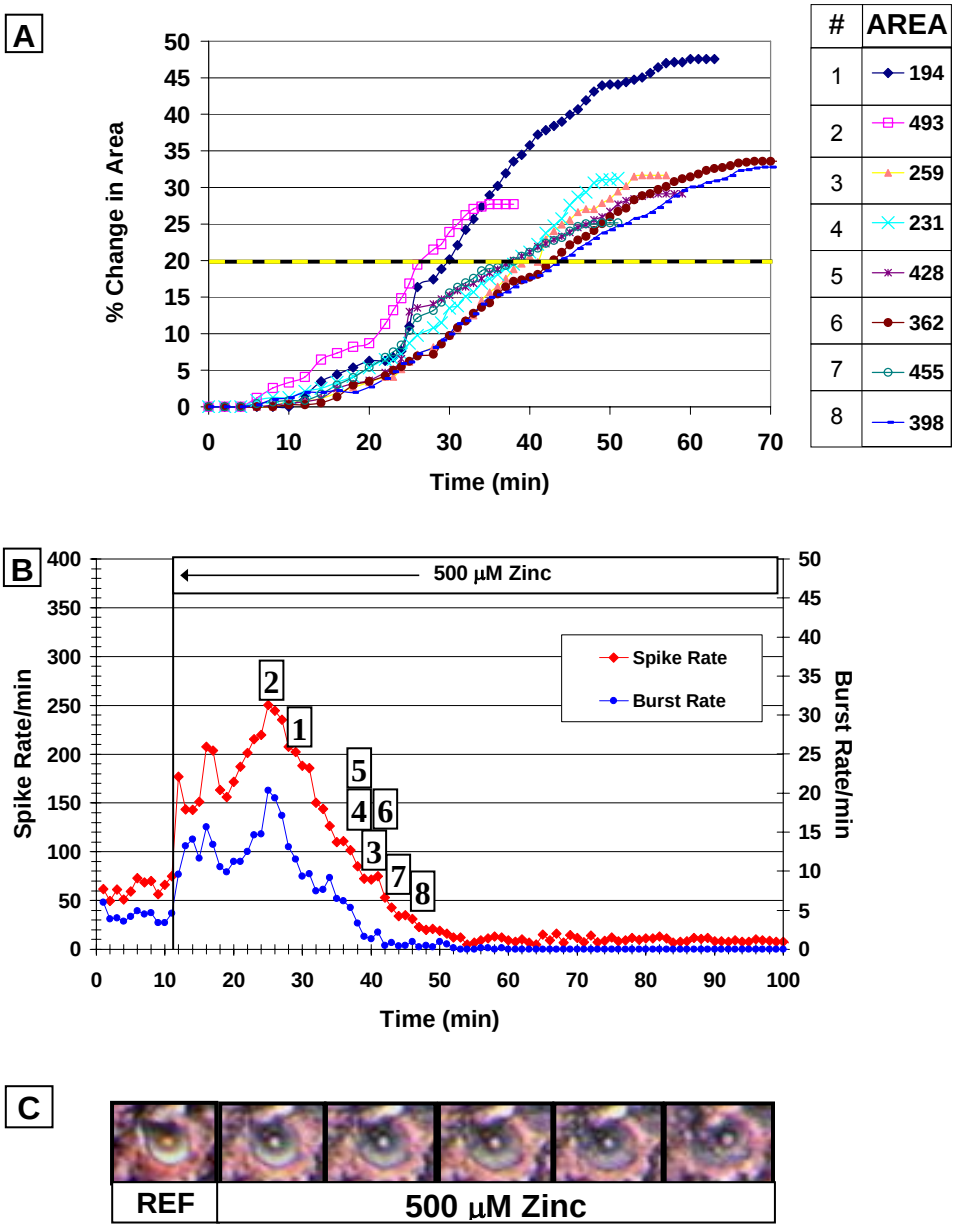

Figure 15. Percent changes in areas of selected neurons. (A) The change in somal areas from neurons # (1-8) is shown each minute following 500 µM zinc additions until the cell lysed. Initial arbitrary areas of each neuron are shown in the box to the right. Plateaus in percent change in area indicate lysing of soma. Dotted line represents 20 % cell swelling. (B) Network activity of the culture in which neurons 1-8 were observed. Boxes indicate the occurrence of 20% swelling of neurons (1-8) during the experiment. (C) Consecutive images shown of a swelling neuron before and after 500 µM zinc application to culture.

3.5 Partial Protection of Networks by Activity Suppression or With Early Removal of Zinc

The irreversibility of activity loss was established in over 40 experiments. Medium changes after zinc-induced termination of activity were never observed to allow even partial recovery. In order to determine the effect of spontaneous activity on zinc toxicity, we conducted three experiments with tetrodotoxin (TTX) at concentrations that blocked all action potential traffic in the networks (200 nM) and four experiments with lidocaine (250 μM). For quantification of protection, we used exposures to 500 μM zinc acetate for 55-60 min, which assures no recovery (Fig. 17A). However, when activity was stopped before zinc application, partial recovery was possible. Fig. 17 (B, C) shows examples of network responses in the presence of these compounds and 500 μM zinc acetate. Zinc was added 10 min after the compounds had blocked all activity and was left on the cultures for 60 min. The treated cultures revealed an immediate and rapid recovery of activity in terms of spike production and active units. Thereafter, the network activity decayed slowly with time. Maximum activity, regained after two medium changes (MC x2), varied greatly in each experiment conducted (Table 3). Note that cultures which regained higher network activity after medium changes required more time to reach 90% network activity loss (Table 3). These experiments represent an indirect blockage of entry routes and demonstrate that despite suppression of all action potential traffic, lethal zinc toxicity still develops. Experiments were done in serum and albumin free medium.

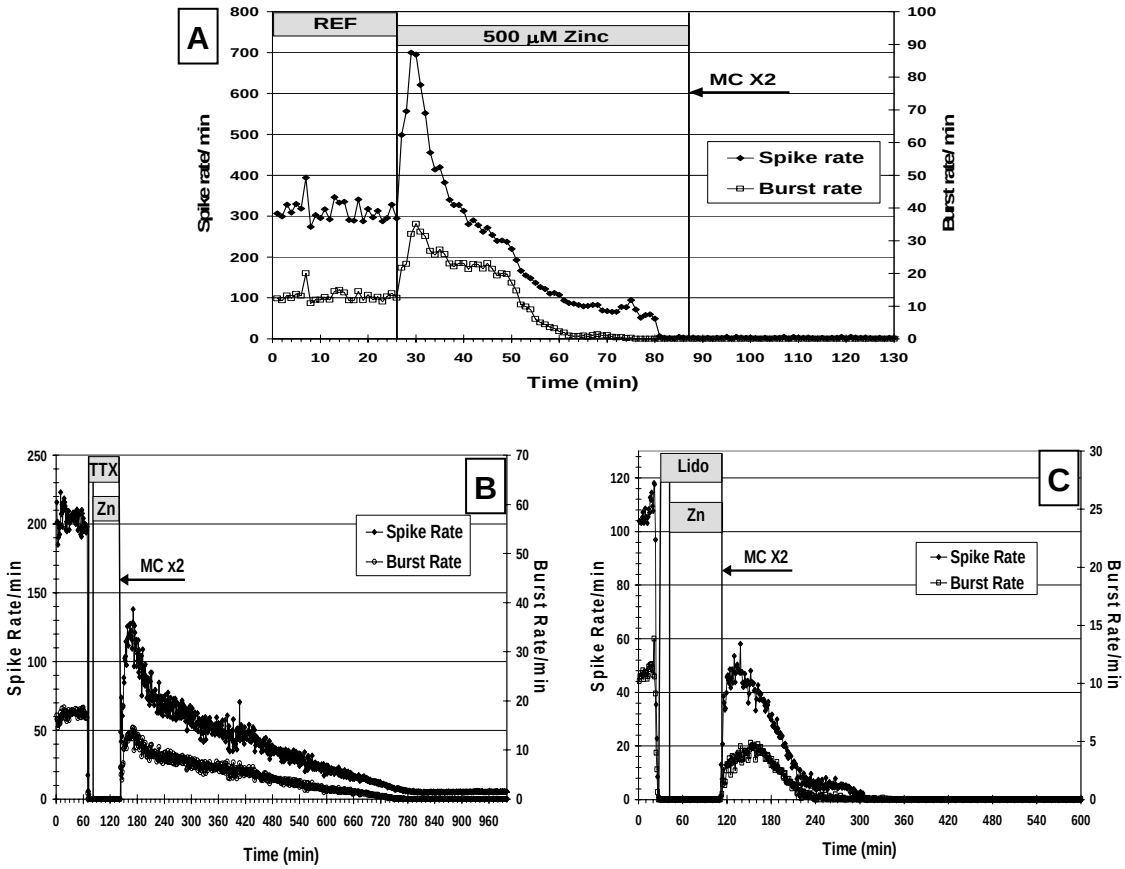

Figure 17. (A) Mean spike and burst production per minute of a network exposed to 500 μM of zinc acetate for 60 min. Recovery of activity after two medium changes (MC x2) is not possible (n=3). (B & C) Acute temporary protection against zinc toxicity with the sodium channel blockers tetrodotoxin (n= 3) and lidocaine (n=4). Plots show real time network activity in terms of average number of spikes and bursts recorded per minute. Acute protection is evident although complete recovery is not achieved and delayed activity decay follows. Zinc acetate (500 μM) was added within 10 min after the compound additions and suppression of spontaneous activity and was left on the networks for 60 min. Ref: reference activity.

Table 3. Summary of Lidocaine and TTX experiments showing the maximum (max) percent of revival and time (min) to 90% activity loss after medium changes.

Lidocaine			TTX		
EXP	Max % revival	Time to -90%	EXP	Max % revival	Time to -90%
MP141	45	121	MP135	167	440
MP183	19	40	MP140	58	90
MP184	38	64	MP153	143	415
MP213	250	125			

In order to determine the transition time from reversible to irreversible damage, we examined responses to early removal of zinc at the IC50 and IC90 times with two medium changes after exposure to 500 μM zinc (Fig. 17). To determine if network were still physically capable of generating spontaneous activity, they were disinhibited with 40 μM bicuculline. Removal of zinc at the IC50 time resulted in activity decay and loss of activity for several hours, but without cellular necrosis (n=2). Fig. 17A shows a quiescent culture that was reactivated with bicuculline. This may demonstrate functional neurotoxicity due to cell stress and partial damage. Removal of zinc at the IC90 time (Fig. 17B) did not reactivate the networks even in the presence of bicuculline (n=2). Morphological observations showed extensive cellular necrosis. All experiments were done in serum and albumin free medium.

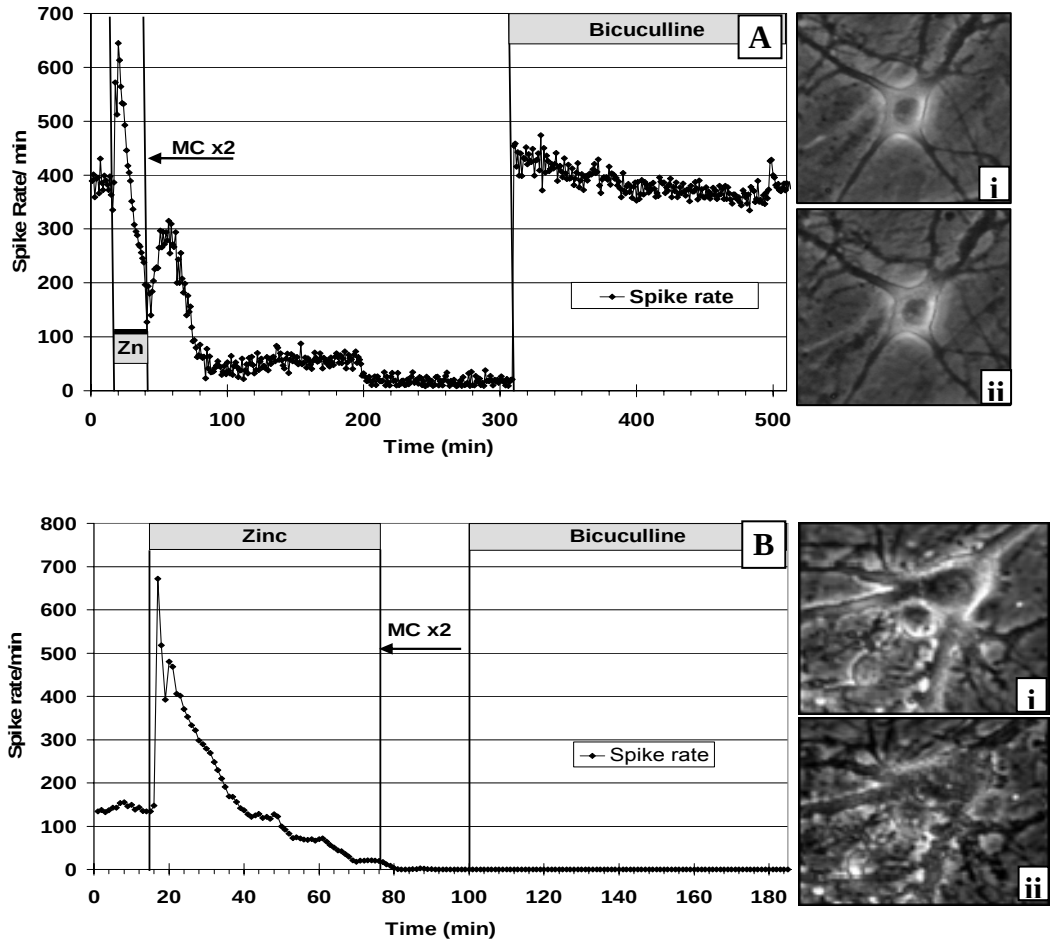

Figure 17. Removal of zinc at IC50 and IC90. (A) Reference activity at 400 spikes per min was recorded before the addition of 500 uM zinc (18 min). After the addition of zinc, a swift decay was observed following a regular excitation phase. When the network reached 50% activity loss, zinc was removed by two medium washes (MC x2). Application of 40 uM bicuculline at 310 min showed recovery of activity to the reference state (n=2). (i) morphology of neuron before zinc application (12 min) and (ii) the same neuron after bicuculline application (320 min). (B) Removal of zinc at 90% activity loss prevented activity recovery. Network did not respond to 40 uM bicuculline (n=2). (i) morphology of neuron before zinc application (10 min), (ii) the same neuron after bicuculline application (120 min).

3.6 Identification of Predominant Entry Pathways for Zinc and Protection of Neurons via Systematic Blockage of Ion Channels

The identification of zinc entry routes have been mainly investigated in depolarization-induced cultures, mainly by KCl additions of up to 50 mM (Sheline et al., 2000; Sensi et al.,1997). However, the understanding of zinc entry pathways is important under normal conditions. The main entry routes for zinc have been suggested to be the calcium channel linked NMDA receptor, calcium permeable AMPA receptor, and the L and N-type voltage gated calcium channels (Sensi et al., 1997, Marin et al., 2001). In order to investigate the predominant entry pathway of zinc into the neuron, the recovery of spontaneous activity was analyzed following entry blockage and toxic zinc application. These receptor linked ion channels, suggested to be entry pathways, were blocked individually prior to the addition of a toxic dosage of zinc (500 μM). Two to three consecutive medium changes were then conducted after 60 minutes exposure and network activity was compared to the reference activity. Verapamil was used to block the L-type voltage gated calcium channels and SNX-111 to block the N-type voltage gated calcium channels. To block the passage of zinc through the calcium permeable NMDA receptors, $MgCl_2$ was applied to the cultures and NBQX was used to inhibit AMPA receptors. The entry route blocker which provides the most protection by presenting the greatest and most continuous network activity recovery is then presumed to be the main entry route for zinc under normal spontaneous conditions.

3.6.1 Blockage of Zinc Entry through NMDA Channels

When zinc is exposed to neurons either by release from the presynaptic neuron or by external application, it is able to enter the postsynaptic neuron via the calcium

permeable NMDA channel. In order to observe the protective effects of blocking this channel, 10 mM $MgCl_2$ was added to the culture medium prior to the addition of 500 μM zinc. The application of $MgCl_2$ completely inhibited the culture's spontaneous activity. After the addition of zinc, one hour was allowed to elapse before the replacement of two medium changes. Network activity recovery was then measured and compared to the native activity. In this case where the NMDA channels were blocked prior to zinc application, activity revival was detected immediately following the medium change for 15-30 min, a drop in activity was detected, and consecutive death resulted (Fig 18).

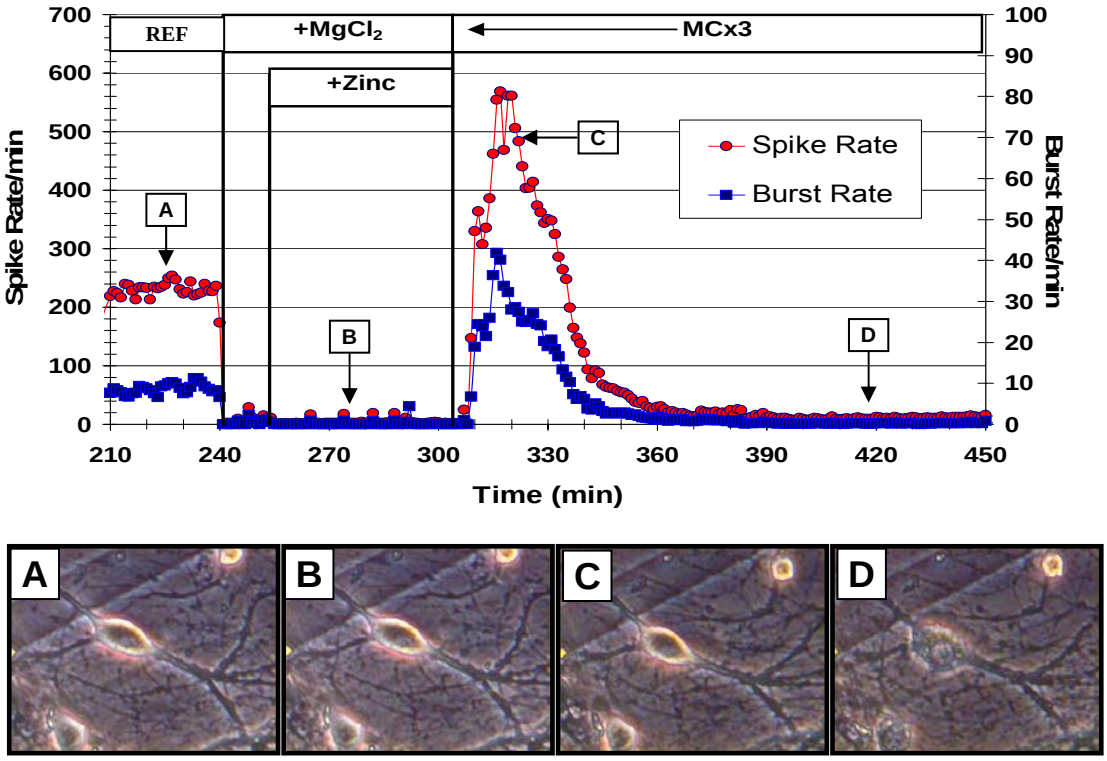

Figure 18. Reference activity is shown for a FC culture from time 210 to 240 (ref). $MgCl_2$ (10 mM) is added at 240 min resulting in complete inhibition of the network activity. At 255 min zinc (500 μM) is applied and left on for 1 hour until 3 consecutive medium changes are taken out at time 305. Activity is regained after the medium changes peaking at 200% of the reference activity in 20 minutes following a rapid loss of activity and cell death. Images (A-D) of the same neuron are shown at different times during the experiment (n=2).

Table 4. Summary of values obtained from experiments in which $MgCl_2$ was used to block the NMDA receptor entry route for zinc. Maximum activity revival is shown for each experiment to indicate the percentage of network activity that was regained after medium changes compared to the reference activity. The time to 90% activity loss after the medium changes is also shown.

Exp	Maximum % activity revival	Time to -90% (min)
MP217	106	180
MP218	55	31
MP236	242	58
Mean ±SD	134 ± 97	89.7 ± 79.4

3.6.2 Blockage of Zinc Entry through AMPA Channels

Another possible route for zinc to enter the neuron is through the calcium permeable AMPA channels. NBQX (20 μM) was used to block AMPA receptors. Unlike the addition of $MgCl_2$ or verapamil which result in total network activity inhibition, addition of NBQX did not inhibit network activity but slowed down bursting with higher coordination. A successive application of 500 μM zinc caused the network activity to decay. Even if medium changes were taken out one hour after incubation with zinc and NBQX, the network activity still continued to decrease until the culture died (n=5) as shown in Figure 19. The time it took cultures to lose 50% and 90% activity after zinc application with NBQX pretreatment were compared to the same reductions in normal medium (Table 5) and no statistical difference was detected (one-sample and unpaired t-test $p<0.05$) (Fig 20). Hence, this shows that pretreatment with NBQX did not prevent zinc neurotoxicity and therefore could not be considered the main entry route.

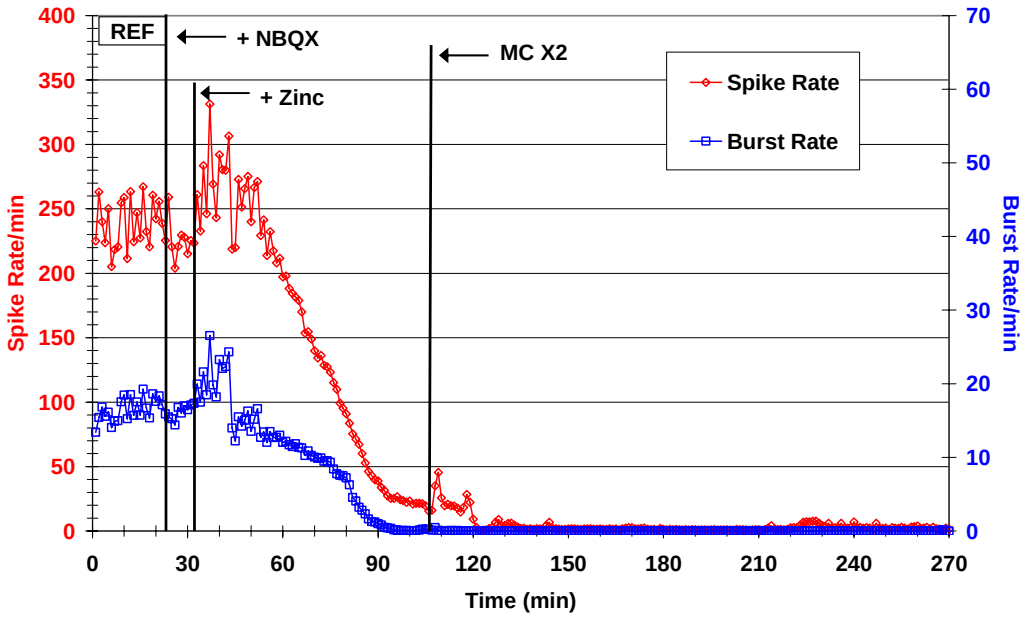

Figure 19. (A) Reference activity (REF) is recorded following the addition of 20 μM NBQX at 23 min. 500 μM Zinc is then applied at 32 min following two consecutive medium changes at 105 min. Network activity decay is continued until all activity is lost. (n=5). (B) The time to 50% and 90% activity loss in FC cultures is shown when exposed to 500 μM zinc, with or without 20 μM NBQX pretreament.

Table 5. Summary of network activity loss experiments from Figure 20. The time (min) it takes for each network to lose 50% and 90% of its activity is shown.

EXP	-50%	-90%
mp110	24	45
mp169	32	53
mp214	20	43
mp238	28	55
mp239	24	45
Mean ± SD	25.6 ± 4.6	48.2 ± 5.4

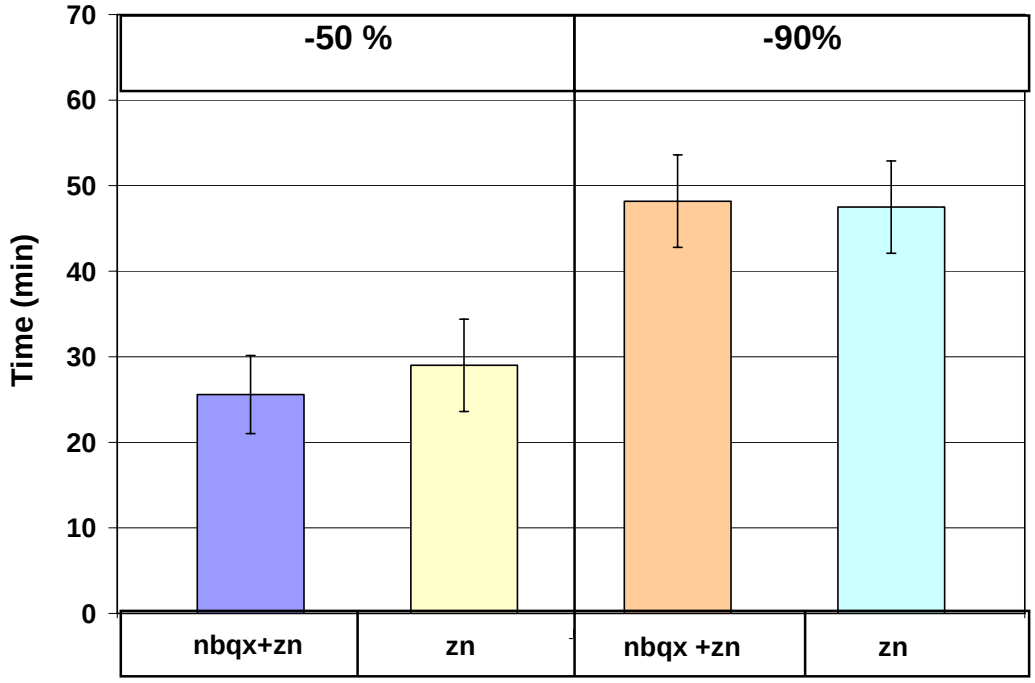

Figure 20. The time (min) to 50% and 90% activity loss in FC cultures is shown when exposed to 500 μM zinc with or without NBQX pretreatment. (n=5). (standard deviations are shown with error bars.) Statistical significance was not detected between values (one sample and unpaired t-test, $P<0.05$).

3.6.3 Blockage of Voltage Gated Calcium Channel Entry

It has been suggested in literature that voltage gated calcium channels also provide an entry pathway for zinc into the neuron (Sheline et al., 2002). The two primary VGCCs which play a role in zinc entry are the L and N types (ibid). Verapamil was used to block the L-type VGCCs and SNX-111 was used to block the N-type VGCCs. Verapamil or SNX-111 were pre-applied to the culture before the addition of 500 μM zinc and left on for one hour. Three medium changes were performed and observations were made to evaluate the amount of activity regained or lost comparing to reference activity. The pre-application of 80 μM verapamil and subsequent exposure of 500 μM zinc to the culture for 1 hr resulted in complete activity revival and full protection from

zinc neurotoxicity (Fig. 21a), however exposure to more than 1hr resulted in total death. The pretreatment of the N-type calcium channel blocker, SNX-111 resulted in partial protection and delayed cell death (Fig. 22).

Table 6. Summary of experiments in which cultures where exposed to zinc and verapamil for 1 hr. The time (min) recorded after the three medium changes is shown for each experiment. The % network activity remaining at time of experiment termination is shown. The activity is compared to the reference activity.

Exp	Recording period after mcx3 (min)	Activity at exp termination (%)
MP143	250	100
MP233	380	245
MP234	600	200
MP235	60	150

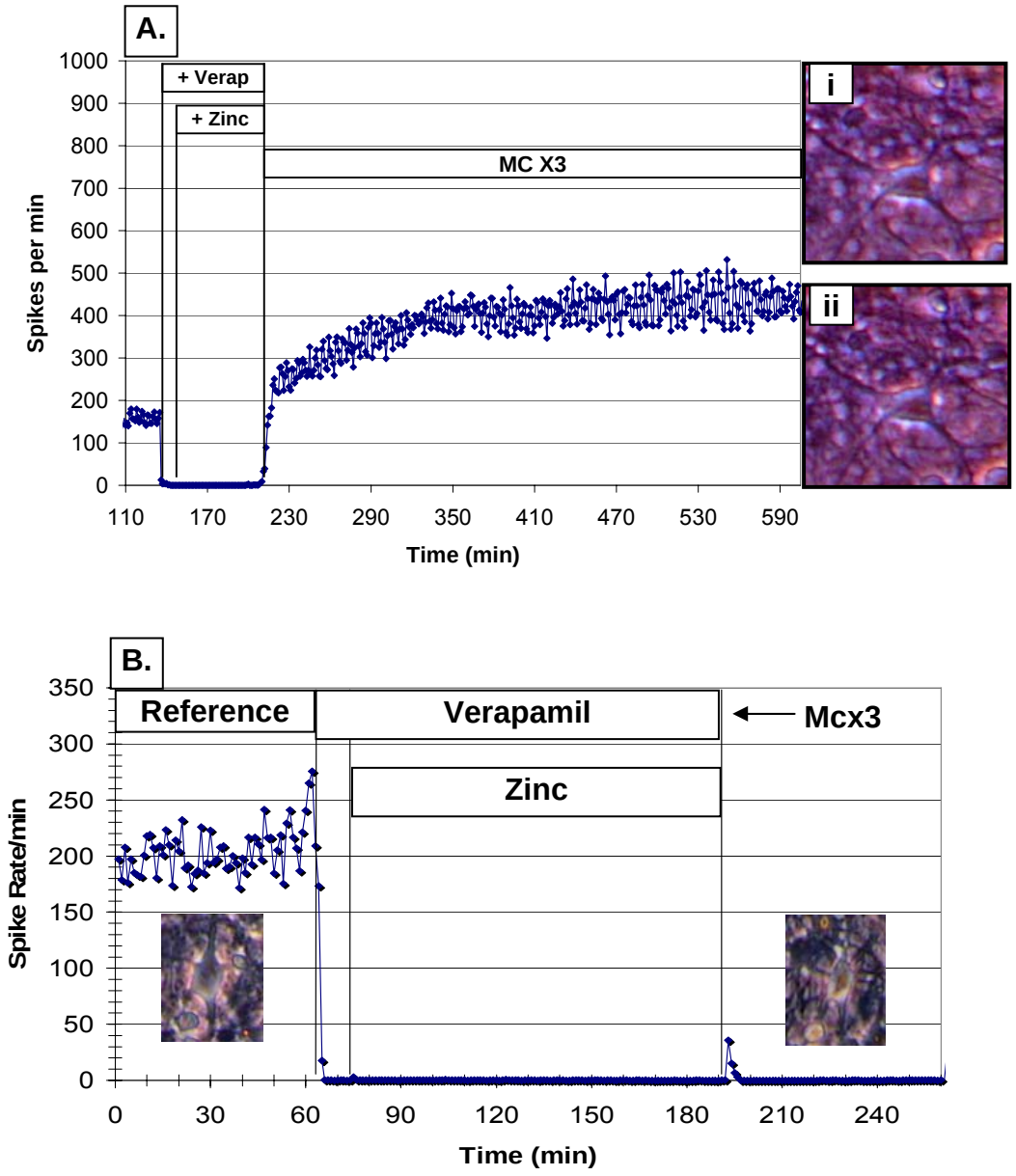

Figure 21. (A) 80 μM verapamil was applied to the culture at 130 min and a consecutive application of 500 μM zinc was given at 140 min. Medium was replaced 3 times (mcx3) at 200 min to assure complete removal of added compounds. Reference activity (R) is recorded for 20 min. (i) neuron before zinc and verapamil are applied and (ii) was the same neuron at 590 min. (n=4) (B) 80 μM verapamil was added to the culture following 60 min of reference activity. Zinc (500 μM) was applied at 73 min and medium was replaced three times (mcx3) at 191 min. Image of the same neuron is shown at 30 min and 225 min (n=3).

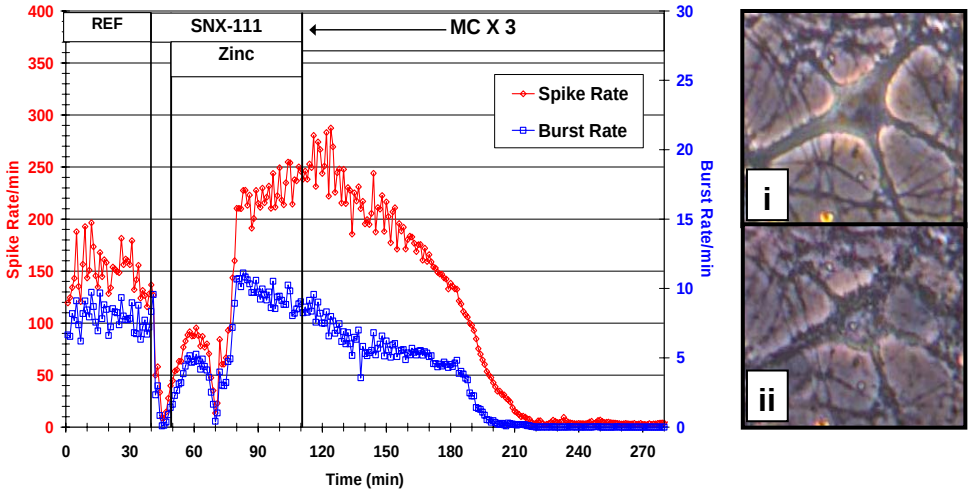

Figure 22. Partial Protection against zinc toxicity via blockage of N-type calcium channel. Culture was treated with 75 μM SNX-11 at 40 min and 500 μM zinc was applied at 70 min then washed out three times at 132 min. Ref: reference activity. Image of neuron in culture at reference activity (i) and at 270 min (ii).

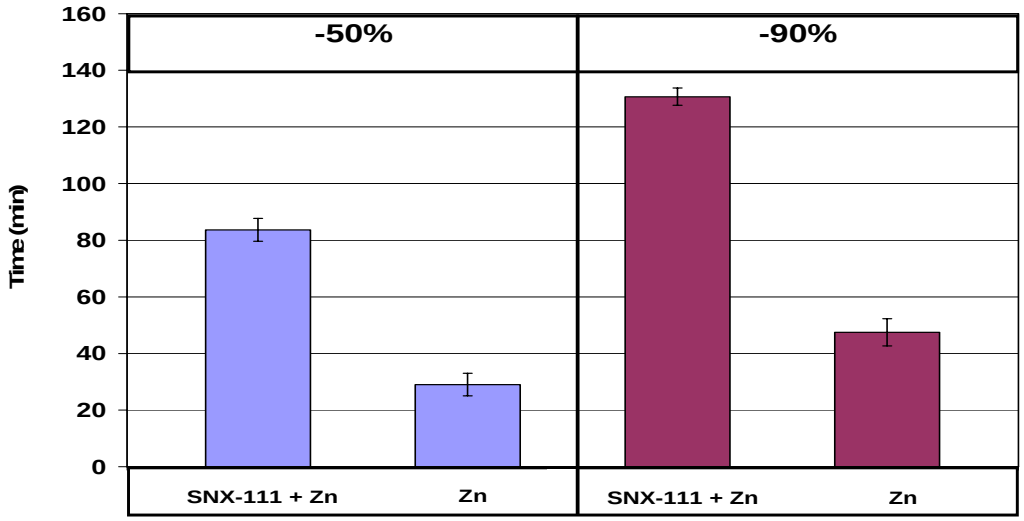

Figure 23. The time to 50% and 90% activity loss in FC cultures is shown when exposed to 500 μM zinc with or without 75 μM SNX-111(n=3). The value obtained indicating the time to 50% activity loss in cultures treated with only 500 μM zinc is the mean of all experimental values (standard deviations are shown with error bars). Statistical significance was detected using both one-sample and unpaired t-test ($p<0.05$).

The pre-application of SNX-111 did not result in an immediate and complete activity inhibition as seen with the application of verapamil, nor did it result in complete protection against zinc neurotoxicity. The pretreatment of cultures with SNX-111 did result in partial protection considering that it took more than twice the amount of time to lose 50% and 90% activity when compared to cultures which had only zinc added (Fig. 21). However, complete network activity decay and consecutive cell death did occur in these experiments.

Table 7. Summary of values showing the amount of time (min) it took to lose 50% and 90% network activity in experiments pretreated with SNX-111.

EXP	-50%	-90%
mp246	80	130
mp247	88	134
mp248	83	128
Mean ± SD	83.7 ± 4	130.7 ± 5.1

Table 8. Summary of 1 hr protection via blockage of entry routes.

Entry Route	Entry Route Blocker	Time to 90% activity loss after MC X3 (min)
NMDA	MgCl2 10mM n=3	58, 31, 180 (highly variable)
AMPA	NBQX 80 μM n=5	0 (no protection)
L-Type VGCC	Verapamil 80uM n=4	Protection
N-Type VGCC	SNX-111 75 μM n=3	130, 128, 134

The greatest protection in these cultures was observed when the L-type calcium channel route was blocked via verapamil. N-type calcium channel and NMDA receptor blockage did also provide partial protection. But AMPA receptor blockage did not provide any protection against zinc toxicity.

3.7 Novel Entry Pathway for Zinc

In this section the likelihood of zinc entering through the chloride channel linked GABA receptors was studied. Enhanced and rapid cell death was observed when 15 μM Muscimol, a GABA receptor agonist was applied to the cultures before a toxic dosage of zinc (300 μM) as seen in Fig 24.

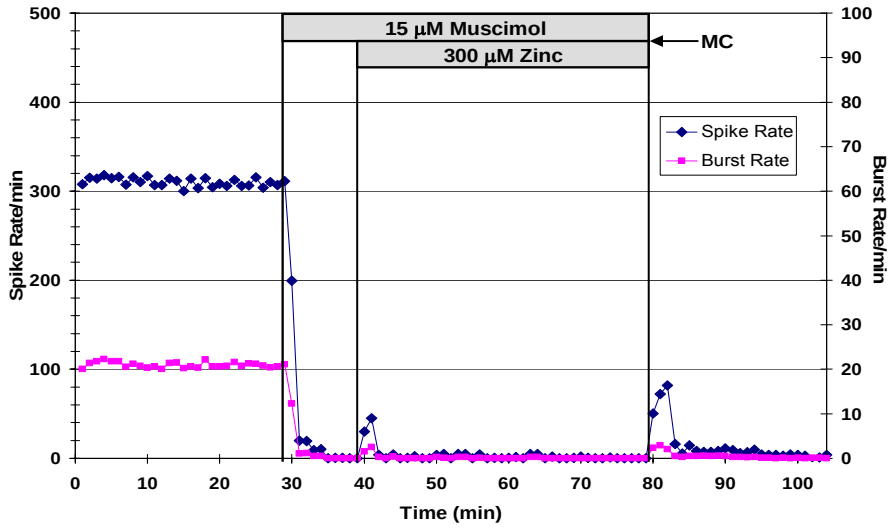

Fig. 24 Stable reference activity (0-28 min) was shut off by 15 μM muscimol followed by the addition of 300 μM zinc. Two full medium changes (MC) showed no recovery of the reference activity (n=3).

This study suggested that pretreatment of cultures with Verapamil and then zinc (≤ 500 μM) for one hour resulted in complete protection against zinc toxicity (fig 21).

When muscimol and verapamil where applied to the culture prior to a toxic dose of zinc no cell/activity revival was observed after medium changes, suggesting that the chloride channel linked GABA receptor to be an entry pathway for zinc.

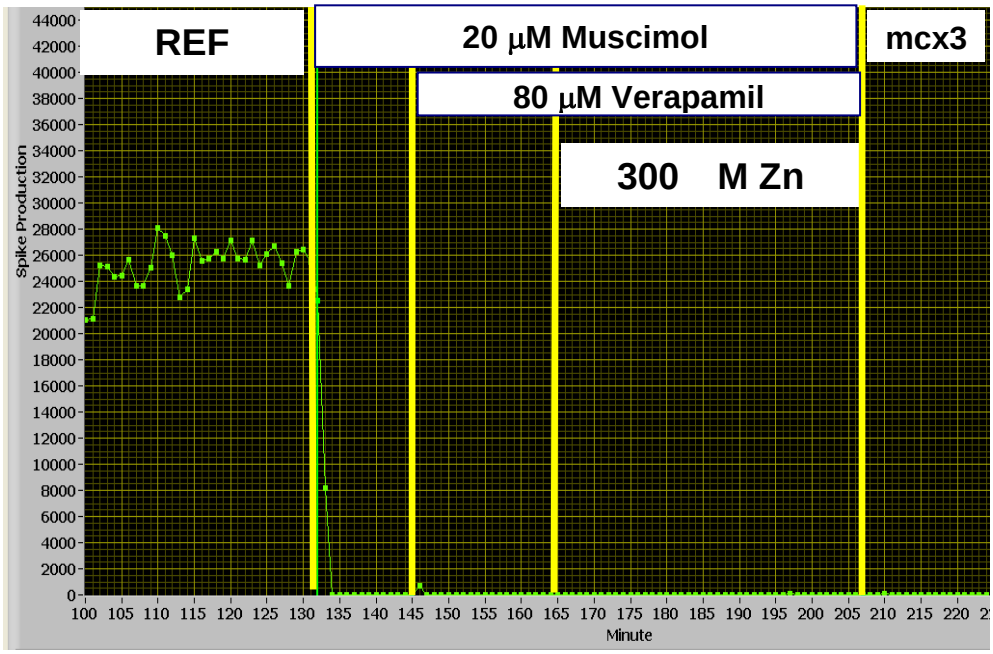

Fig. 25. Protection Suppressed with addition of muscimol. Culture was initially treated with verapamil (80 μM) and muscimol (20 μM) was added 20 min later followed by the addition of 300 μM zinc. Three medium changes (mcx3) were taken out in 40 min. (n=3)

CHAPTER 4

DISCUSSION

The cytotoxicity of zinc is established as a phenomenon, but has been based primarily on morphological observations and measures of cell death (Choi et al., 1988; 1992; Koh et al., 1996). The mechanism by which zinc exerts its toxicity is controversial. Koh et al. (1996) and Kim et al. (1999) suggest oxidative stress whereas Sheline et al. (2000) favors failure of energy production due to mitochondrial damage. Capasso et al. (2005) recently showed that mitochondrial damage plays a role in zinc induced neuronal cell death. This is accompanied by extra-mitochondrial production of reactive oxygen species and disruption of metabolic enzymatic activity, eventually leading to neuronal injury (ibid). However, there appear to be multiple entry pathways and the temporal aspects of entry and subsequent cellular damage were not quantified. Further, influences on the electrophysiological function of neuronal ensembles were unknown and the possibility of functional neurotoxicity in the absence of cytotoxicity was not considered previously. Therefore, quantitative analyses using multichannel electrophysiological techniques that can monitor the temporal evolution of toxicity in a neuronal network can provide important dynamic information to the field of zinc toxicity. As shown in this study, such an approach provides additional information in terms of activity changes, points of reversibility, and quantitative data based on the readout of system spike production and burst patterns. Linkage between morphological deterioration and loss of activity can also be established. Further, in the culture environment, the measurement of free zinc is facilitated.

Despite the clear warning signs of toxicity, zinc exposure in industrialized nations is increasing. Zinc is found in almost every skin powder, is added to most vitamin supplements, and is found in such diverse products as dental adhesive, sun screens, nasal sprays, and potions designed to boost the immune system. To this must be added environmental exposures, as zinc is found in automobile tires, paint, batteries, galvanized metals, and in some new nanomaterials that are emerging rapidly without systematic toxicity analyses. Inhalation of zinc compounds, mainly zinc oxide fumes, can lead to a condition known as "metal fume fever". The symptoms include headache, altered taste, nasal passage irritation, cough, rales, fever, weakness, hyperapnea, sweating, pains in the legs and chest, reduced lung volume, and leukocytosis (ATSDR, 1988; Bertholf, 1988).

Compared to mercury (Gopal, 2002) and lead (unpublished observations), zinc causes similar rapid deteriorations of network activity at high concentrations. However, the mechanisms are different, as cell swelling and lysis were not observed in response to mercury intoxication (Gopal, 2002). The observed osmotic swelling of neurons in the presence of zinc acetate is compatible with a blocking of mitochondrial function and impairment of membrane ionic pumps. Neuronal cell rupture in media has been reported (Choi, 1988) and observations in our laboratory of neuronal lysing in normal media were frequent. Although the time to activity loss and cell death is a function of concentration (Fig. 13; equations 1 & 2), neuronal swelling is seen already at 20 μM whereas lysing is observed generally above 50 μM zinc acetate. It is interesting that Choi et al. (1988) reported an ED_{50} of 600 μM (total zinc) 15 min after zinc application for cortical cultures using LDH assays. This evaluation correlates with our time for 50%

activity reduction at 600 μM (equation 1). However, at this time, cells do not show major deterioration and more than 90% of the units are still firing, albeit at a reduced level.

We observed that networks responded to all zinc concentrations, starting at 20 μM zinc acetate, with initial excitation followed by irreversible activity decay in the absence of medium changes. This was seen when experiments were carried out in serum and albumin free medium (see Fig. 13). If zinc was added to cultures in medium containing 5% serum, only concentrations including and above 175 μM were effective, indicating that the serum components and albumin bind zinc and protect cells. This agrees with the work of Lin et al. (2005), which suggested that albumin is protective of zinc-induced neurotoxicity of cultured rat cerebellar granule neurons. In our studies, activity could be restored by medium changes at the IC50 time for 500 μM zinc exposure in serum and albumin free medium (Fig. 17). The time when partial recovery can be achieved is strongly concentration dependent. Critical levels of zinc appear to enter the cytoplasm between IC50 and IC90 times. At 500 μM this occurs within 12 minutes, although at 20 μM zinc that time gap is 220 minutes (equation 1). Both the amplitude and duration of the excitatory phase are also concentration-dependent but, at high concentrations, a rapid silencing of units truncates the excitation phase. It has been proposed that zinc attenuates the GABA response and thereby elicits hyperexcitability of the neurons (Ruiz et al., 2004; Westbrook and Mayer, 1987). Conversely, it has also been found that zinc acts as an inhibitory neuromodulator as it can selectively block N-methyl-D-aspartate (NMDA) receptors (Christine and Choi, 1990). In patch recording experiments, concentrations of 10-100 μM zinc chloride reduced single NMDA channel conductivity coupled to an increase in channel noise,

suggestive of a fast channel block (ibid). However, our observations show that the excitation dominates at all concentrations tested, indicating that the network effects of possible GABA receptor blocking are stronger than the influences of NMDA receptor inactivation. In addition, the excitation is accompanied by increased burst coordination among channels with enhanced burst period regularity (see Fig. 6B). This is also demonstrated by the reduced variability of the minute means in burst period plots that represent an average across all discriminated units selected for recording (Fig. 6A). In these cultures, such burst coordination and temporal pattern regularization is characteristic of GABA receptor or channel blockage (Keefer et al., 2001 b,c).

The electrophysiological effects of synaptically released zinc and those generated by exogenous loading of zinc by relatively high concentrations appear to have diverse effects. Whereas the former is considered to have anti-excitatory influences because of zinc inhibition of practically all glutamate receptors (Frederickson et al., 2004), higher concentrations of exogenous zinc generate extensive excitation that appears to be terminated only by the subsequent zinc-induced cell destruction. This concentration-dependent paradoxical effect of zinc complicates zinc investigations and mechanistic explanations of observed effects. In this paper we have focused on a exogenous exposures over a large concentration range in order to quantify toxic effects in terms of total zinc acetate added to the cultures. Concentrations applied to cultures which where below 20 μM did not result in any electrophysiological changes and cell death when evaluated for 24 hours. This indicates that the cells have a functional buffering capacity for concentrations that do not exceed 20 μM. Metallothionenes have been suggested to play an important role in this buffering of zinc (Palmiter, 1998). They

seem to play a major role in altering accessibility of free zinc ions for the zinc-binding enzyme group by being able to bind and dispense free zinc ions (ibid). Its been previously implied that application of certain heavy metals like zinc to neuronal cultures causes upregulation of metallothionenes (Palmiter, 1988). Our data agrees with these observations, as it is seen in this study that a high concentration of zinc (200 μM) can be added to culture in very small nontoxic increments such as 10 μM to delay neurotoxicity (Figure 10).

As previously mentioned, the applications of zinc above 20 μM resulted in an excitation phase which was quantified in this study. The observed excitatory phase by itself cannot be held responsible for the concomitant loss of activity and cell deterioration. Such a degree of excitation can be obtained with many pharmacological manipulations that do not result in cell death. Also, the excitatory phase is eliminated in the presence of bicuculline and picrotoxin, but activity decay and cell deterioration is still observed. Consequently, a vesicular release of endogenous zinc does not seem to be the primary mechanism of toxicity. Our data are therefore not directly linked to excitotoxicity but rather to the entry of zinc through channels, which triggers subsequent cellular damage. Certainly, the extensive swelling and frequent lyses of neurons represent observations consistent with mitochondrial damage and associated osmotic swelling due to ion gradient deregulation. Neurons evaluated in frontal cortex cultures were capable of swelling up to 50% of their initial area before they lysed. It was found that the initial area of a neuron is not correlated with the time it takes for it to lyse. Another interesting observation made was that 20% neuronal swelling occurs close to the time when 50% network activity has decayed.

The experiments conducted to show acute, partial protection represent the beginning of a systematic effort to block and possibly rank the efficacy of entry routes. Temporary protection of neurons occurs under conditions of suppressed or blocked activity. It may be assumed that suppressed electrical activity lowers the probability of channel opening and reduces zinc entry. These observations support earlier published data suggesting that a major entry route for zinc is through channels associated with network electrical activity including voltage-gated calcium channels, NMDA receptors, and AMPA receptors (Koh and Choi, 1994; Sensi et al., 1997). This study has also analyzed these main entry routes and suggested the primary entry pathway for neurons in spontaneous, non-depolarized state to be the L-type voltage gated calcium channels due to protection against 500 μM zinc by L-type specific calcium channel blocker, verapamil. However complete protection was only seen when cultures where exposed to verapamil and zinc for 1 hour. Exposures beyond 1.5 hours resulted in cell death. This could indicate the entry of zinc through routes not associated with electrical activity like zinc transporters. Zinc transporters are proteins existing on most cells in the body known to permit both the entry and exit of zinc and sometimes other cations. They are the least understood of all the entry routes in terms of mechanisms and are very difficult to manipulate pharmacologically since they are not known to respond to any drugs presently available.

It has been reported for the first time in this study that chloride channel-linked GABA receptors may provide an entry pathway for zinc into the FC neurons. Zinc has been suggested to bind to the $GABA_A$ receptor (Smart et al., 1994) but has never been implicated as an entry route. The pretreatment of FC neurons with a $GABA_A$ receptor

agonist, muscimol induced a more rapid cell death compared to cultures which had not been pretreated. This implied that opening of the chloride channel allowed more zinc to enter the neurons. Even when tested with the presence of verapamil cells where not spared. Therefore it is strongly suggested that zinc enters FC neurons through chloride channels linked to $GABA_A$ receptors. These findings imply the possibility of enhanced neuronal cell death for persons consuming drugs which act as $GABA_A$ receptor agonists, such as benzodiazapenes or alcohol.

Whether the concentrations used in this study are ever attained in animals even under high environmental zinc exposures is difficult to determine. Binding, compartmentalization, and clearance represent complicated dynamic factors that are not yet clearly defined. However, synaptic concentrations have been estimated to reach 300 μM under strong stimulation or depolarizing conditions (Assaf and Chung, 1984). It is important to quantify the temporal evolution of zinc toxicity on the cellular and small network levels as such toxicity represents a basic dynamic feature that must be defined to support future studies of zinc buffering and clearance, both on the cellular and organismal levels.

Electrophysiological assessments of toxicity, if based on the monitoring of many active units, provide a highly fault-tolerant, quantitative measure that is relatively simple to use. The anticipated technical expansions to multinetwork platforms and robotic cell seeding, maintenance, and testing will result in a major increase in assay efficiency. Primary cell culture will emerge as the preferred core methodology as embryos from a single mouse can seed over 1000 MEAs if different regions of the central nervous system are used. Validation of primary culture as histiotypic assay platforms was

therefore a secondary goal of this investigation. As with many other compounds (Gross and Gopal, 2006; Gross and Pancrazio, 2006), the results reported in this paper with zinc acetate agree well with the literature and provide additional quantitative data on the dynamic aspects of toxicity development.

The better understanding of the temporal dynamics of zinc toxicity may allow application of these finding to a variety of other tissues. Central to such applications is the potential control of tumor growth or elimination. It is possible, that localized high concentrations of zinc can affectively eliminate malignant cells without a major disruption of surrounding healthy tissue. The high zinc buffering capacity of cells can be used to create a sharp gradient between toxic and nontoxic concentrations. It is anticipated that different tissues will show different zinc uptake and toxicity dynamics. However, glandular tumors such as those found in testosterone sensitive prostate cancer, may be highly similar in their response to what has been seen for neural tissue in this study. Therefore, the investigation of zinc toxicity in a variety of different tissues should be highly encouraged.

APPENDIX A

DRUG CONTROLS

Acetate

Zinc was applied to the cultures in the form of zinc acetate. In order to rule out the effects of acetate, 2 mM sodium acetate was added to the culture and no change in electrophysiological activity was observed for about 6 hours (355 min). The osmolarity at reference period (R) was 324 milliosmoles and at termination it was 327 milliosmoles. PH remained unchanged at 7.43.

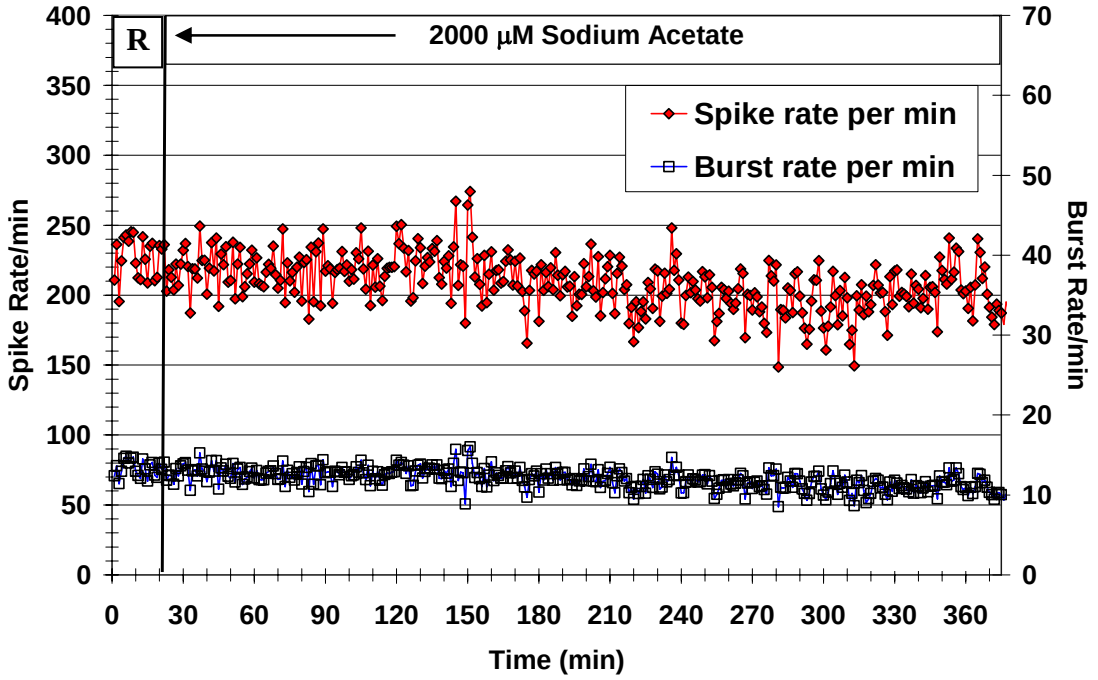

$MgCl_2$

Magnesium Chloride, (8 mM) was preapplied to cultures before the addition of zinc and left on the culture for 60 min to inhibit the NMDA receptors, one route of entry for zinc ions. Medium changes resulted in activity loss and cell death within 180 min. In order to rule out the effects of $MgCl_2$, 8 mM was added to a culture and left on for 60 min resulting in complete activity inhibition. Network activity was regained after two medium changes (MCX2) and observed for 200 min. Osmolarity was 226 milliosmoles during reference activity (REF), 228 milliosmoles during incubation with MgCl2, and 227 milliosmoles at time of termination.

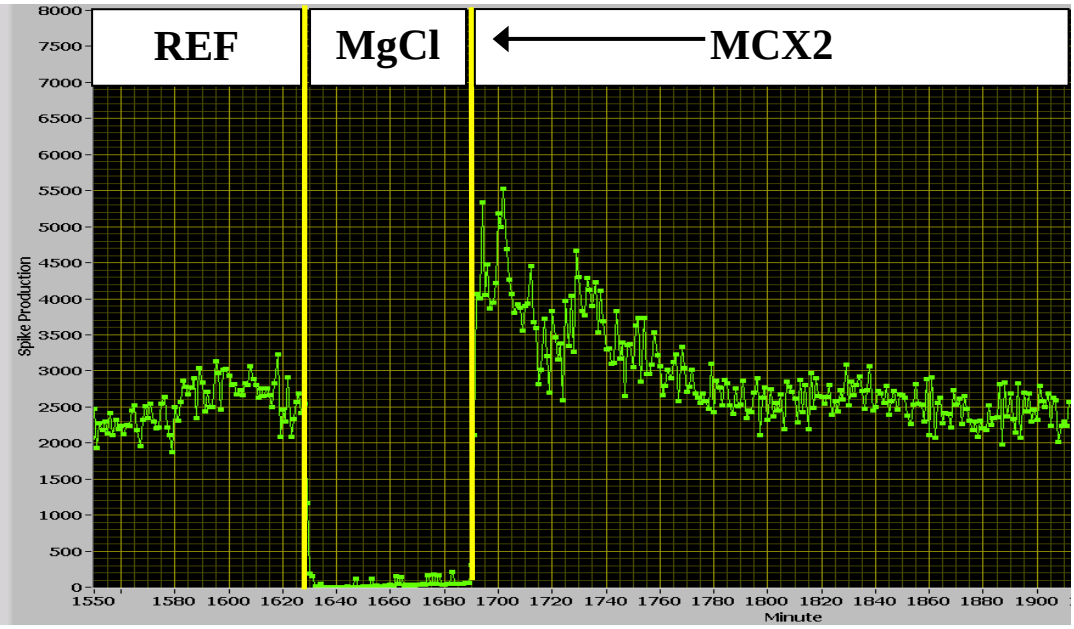

SNX-111

The reversibility of SNX-111 was tested by application of 75 μM (in 25 μM increments at 38, 81, and 162 min) then washed out three times (MC X3) at 222 min showing complete activity revival.

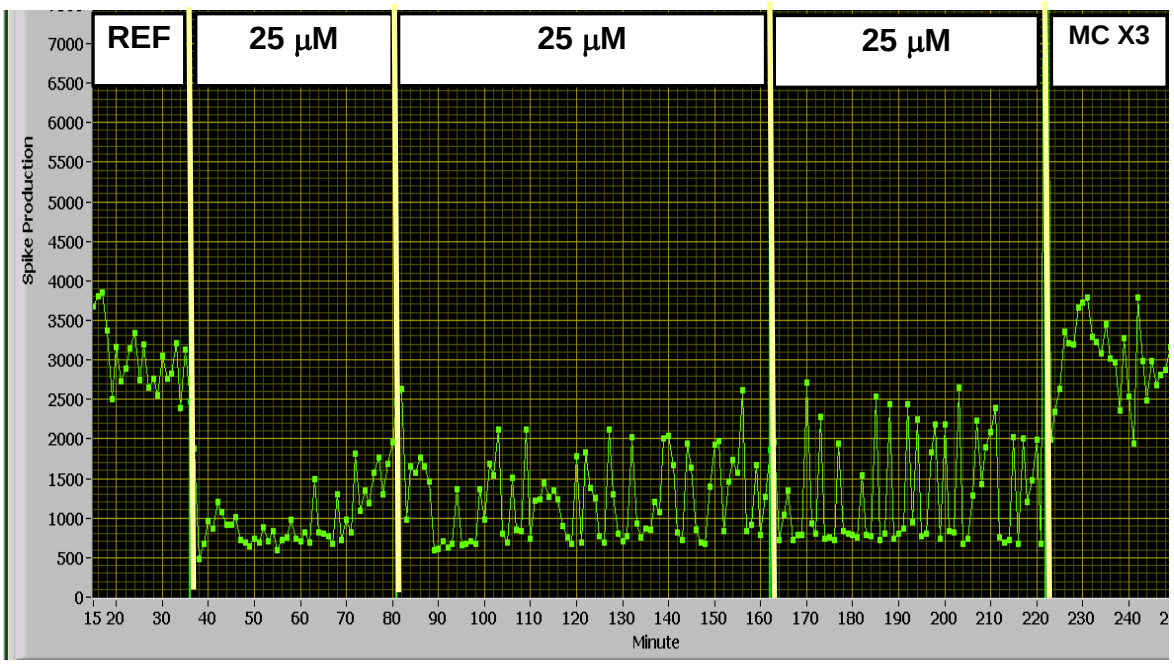

Lidocaine

Reference activity was recorded for 20 minutes following 250 mM Lidocaine application to the culture. This resulted in immediate network activity inhibition. When the culture's medium was changes two times at 96 min, complete network activity was regained hence showing the complete reversibility of lidocaine.

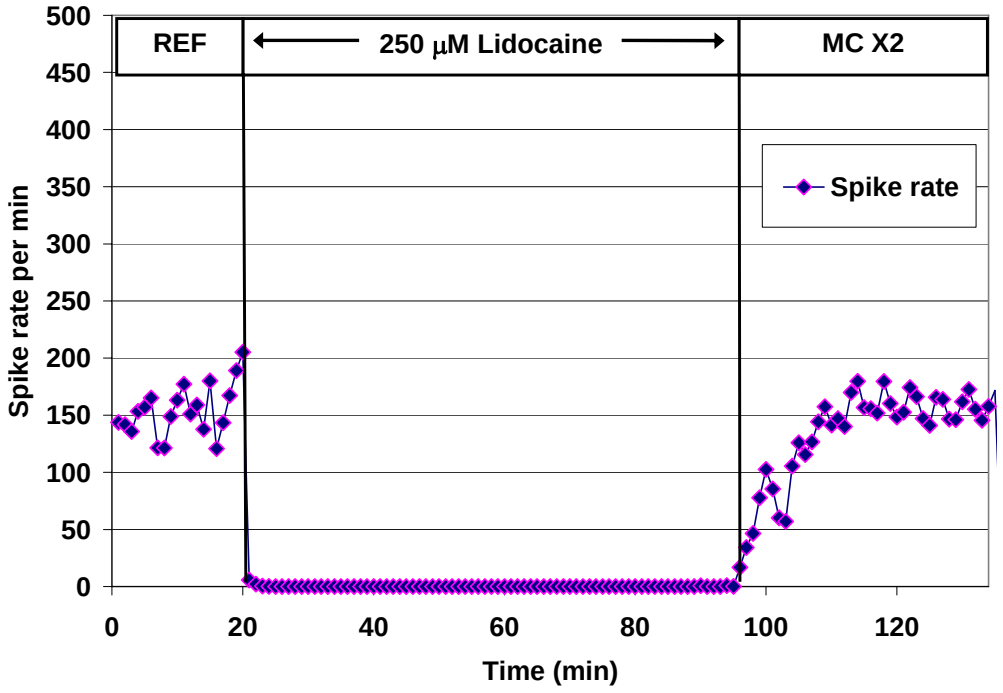

Verapamil

80 μM Verapamil was applied to the culture at 255 min removed via 3 full medium changes at 292 min. This resulted in complete activity (dotted line) & unit revival (straight line) therefore presenting the reversibility of verapamil.

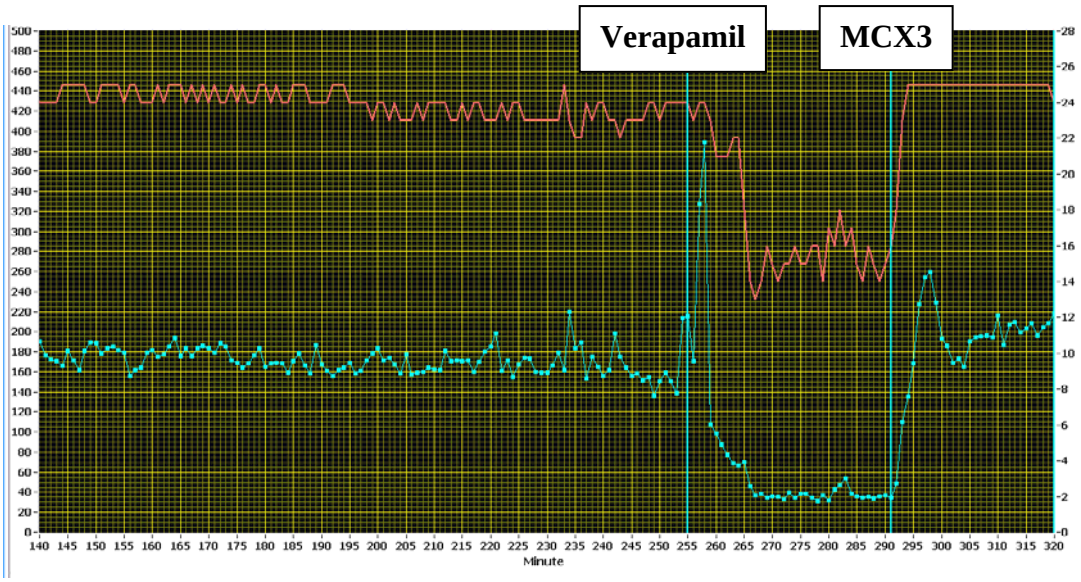

APPENDIX B

FREE ZINC CALCULATIONS

Free zinc calculations in DMEM stock solution are made after additions of various zinc concentration (Courtesy of Neurobiotex). To be aware of how much free zinc is being exposed to the cells after addition of zinc acetate, individual samples of DMEM stock solution (not including cells) containing various concentrations of zinc acetate (10 - 2000 μM) were analyzed by Neurobiotex and sample readings of free zinc were obtained.

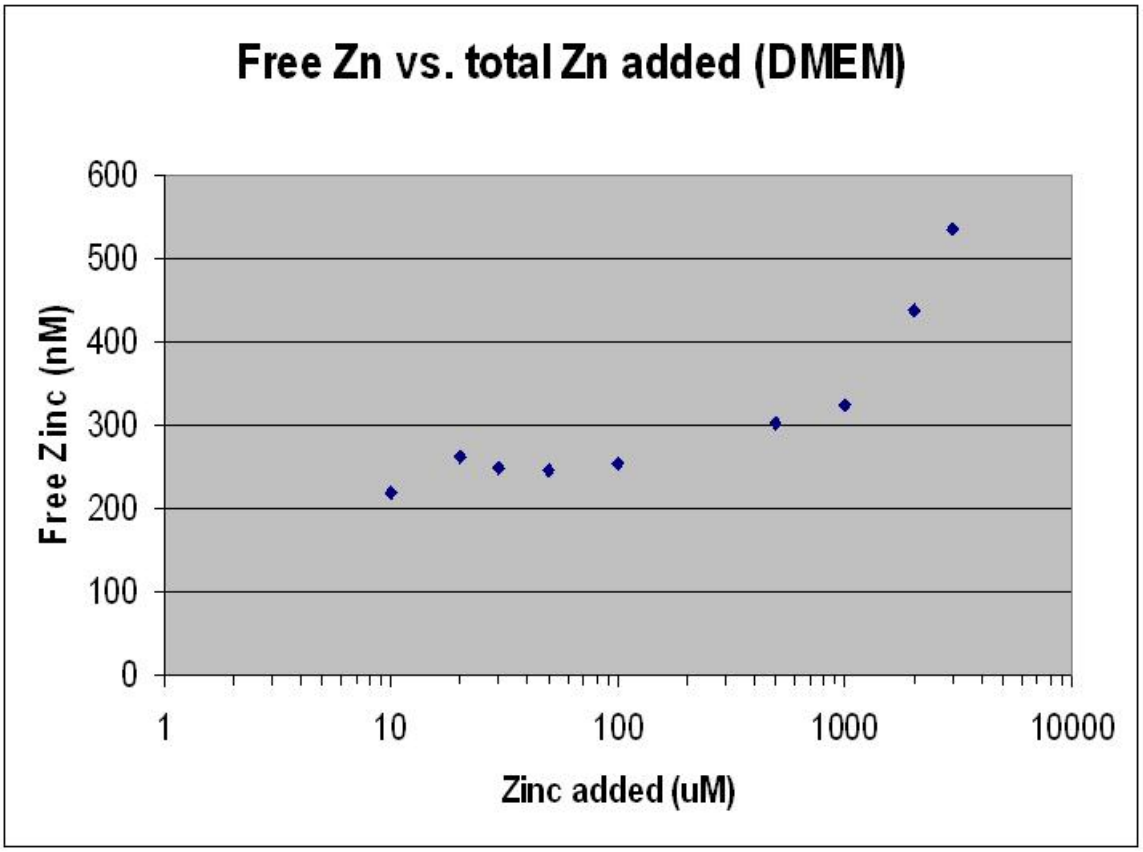

APPENDIX C

CONFIDENCE LIMITS & LINEAR SCALES

95% Confidence Limits for 50% Activity Loss

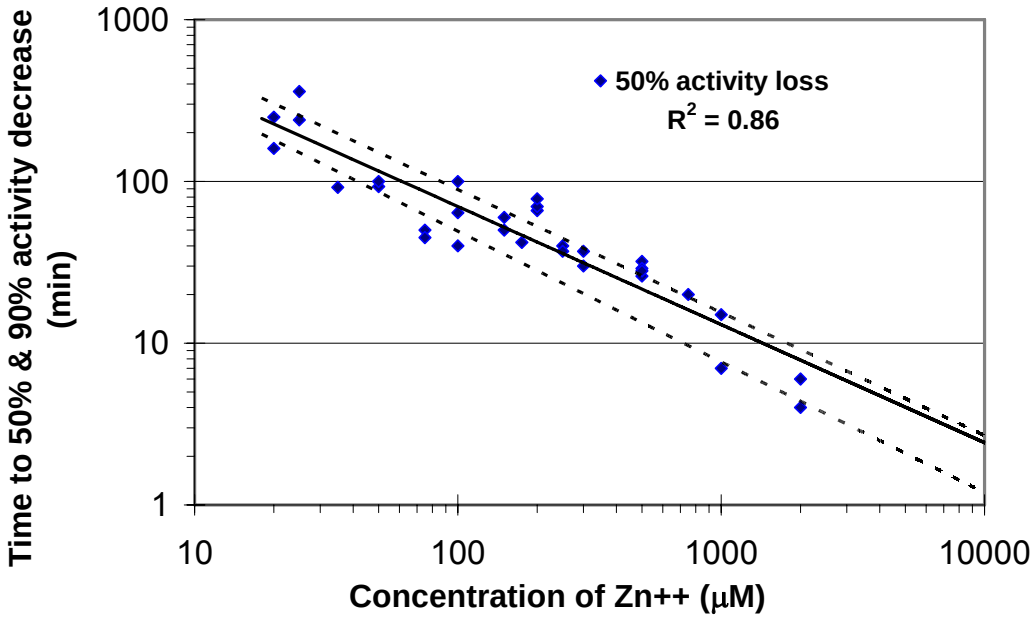

Equations below may be used to find the upper and lower limits for each concentration of zinc applied to a culture (Excel).

Upper Limits: $t = 2951C^{-0.76}$

Lower Limits: $t = 2028C^{-0.81}$

95% Confidence Limits for 90% Activity Loss

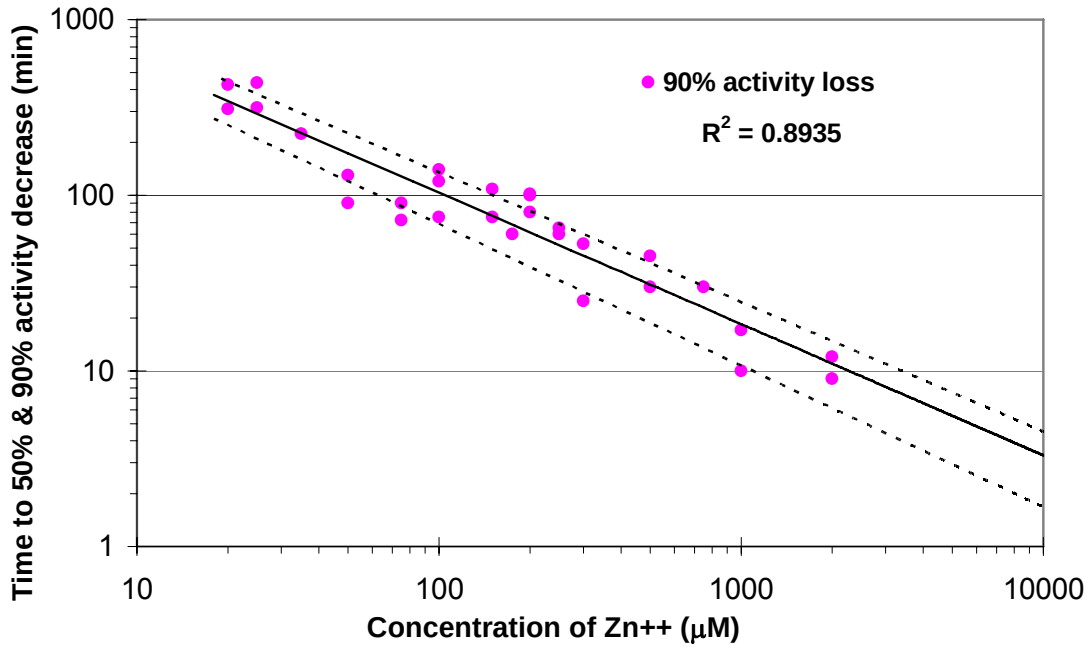

Equations below may be used to obtain the upper and lower limits of each concentration of zinc applied to a culture (Excel).

$$\text{Upper Limits: } t = 4064C^{-0.74}$$

$$\text{Lower Limits: } t = 2794C^{-0.81}$$

50% Activity Loss (linear scale).

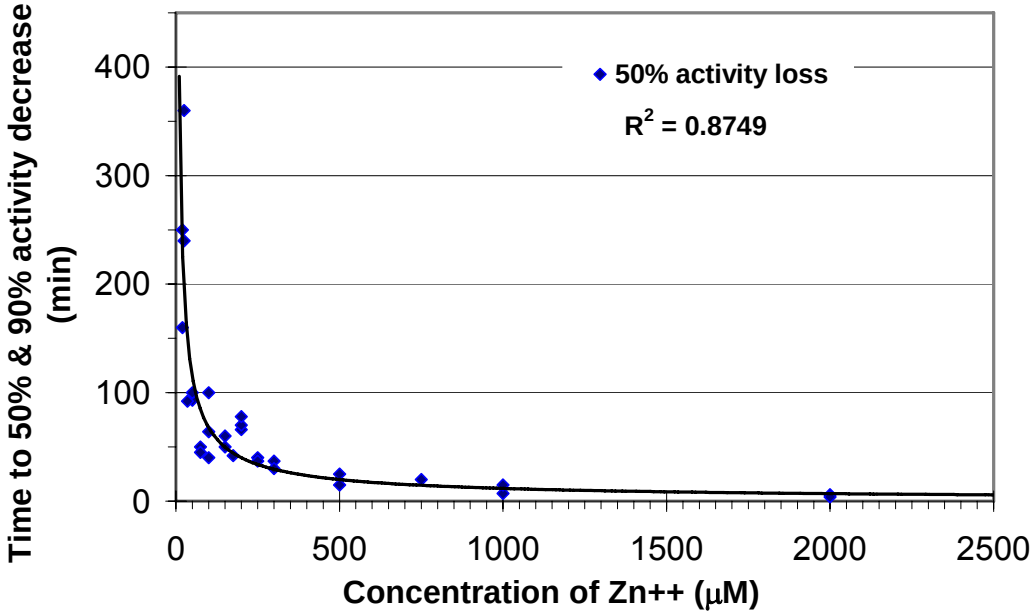

90% Activity Loss (linear scale).

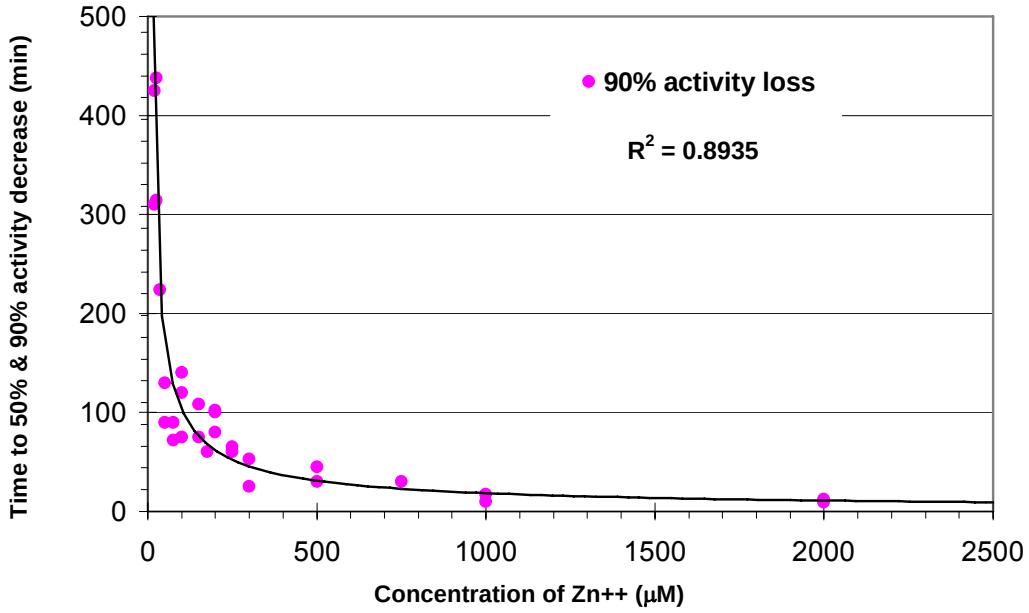

REFERENCES

Adamson I, Prieditis H, Hedgecock C, Vincent R. Zinc is the Toxic Factor in the Lung Response to an Atmospheric Particulate Sample. Toxicology and Applied Pharmacology 1999; 166(2): 111-119.

ATSDR. Draft Toxicological Profile for Zinc. U.S. Department of Health and Human Services, Public Health Service, Atlanta, GA. 1988

Assaf SY, Chung SH. Release of endogenous Zn^{2+} from brain tissue during activity. Nature (London) 1984; 308:734-736.

Bertholf RL. Zinc. In: Handbook on Toxicity of Inorganic Compounds, Seiler HG, Sigel H, editors. New York: Marcel Dekker,1988 (pp. 787-800).

Capasso M, Jeng JM, Malavolta M, Mocchegiani E, Sensi SL. Zinc dyshomeostasis: a key modulator of neuronal injury. J Alzheimers Dis 2005; 2:93-108.

Canzoniero LM, Turetsky DM, Choi DW. Measurement of intracellular free zinc concentrations accompanying zinc-induced neuronal death. J Neurosci 1999 19;(RC31):1-6.

Chen CJ, Liao SL. Zinc toxicity on neonatal cortical neurons: involvement of glutathione chelation. J Neurochem. 2003; 85(2):443-453.

Chen WQ, Cheng YY, Zhao XL, Li ST, Hou Y, Hong Y. Effects of zinc on the induction of metallothionein isoforms in hippocampus in stress rats. Exp. Biol Med 2006; 213(9):1564-1568.

Cheng C, Reynolds IJ. Calcium-sensitive fluorescent dyes can report increases in intracellular free zinc concentration in cultured forebrain neurons. J Neurochem 1998; 71(6):2401-2410.

Choi DW, Yokoyama M, Koh J. Zinc neurotoxicity in cortical cell culture. Neuroscience 1988; 24(1):67-79.

Choi DW. Excitotoxic cell death. J Neurobiol 1992; 23:1261-1276.

Christine CW, Choi DW. Effect of zinc on NMDA receptor-mediated channel currents in cortical neurons. J Neurosci 1990; 10:108-116.

Colvin RA. Characterization of a plasma membrane zinc transporter in rat brain. Neurosci Lett 1998; 247(2-3):147-150.

Colvin RA, Davis N, Nipper RW, Carter PA. Zinc transport in the brain: routes of zinc influx and efflux in neurons. J Nutr 2000; 130(5S Suppl):1484S-1487S.

Colvin RA, Fontaine CP, Laskowski M, Thomas D. Zn2+ transporters and Zn2+ homeostasis in neurons. Eur J Pharmacol 2003; 479(1-3):171-185.

Cousins RJ. Absorption, transport, and hepatic metabolism of copper and zinc: special reference to metallothionein and ceruloplasmin. Physiol Rev 1985; 65:238-309.

Davies NT. Studies on the absorption of zinc by rat intestine. Br J Nutr 1980; 43:189-203.

Davies NT, Nightingale R. The effects of phytate on intestinal absorption and secretion of zinc, and whole-body retention of Zn, copper, iron and manganese in rats. Br J Nutr 1975; 34:243-258.

Desouki MM, Geradts J, Milon B, Franklin RB, Costello LC. hZip2 and hZip3 zinc transporters are down regulated in human prostate adenocarcinomatous glands. Mol Cancer. 2007 Jun 5; 6:37.

Dineley KE, Votyakova TV, Reynolds IJ. Zinc inhibition of cellular energy production: implications for mitochondria and neurodegeneration. J Neurochem 2003; 85(3):563-570.

Ding WQ, Liu B, Vaught JL, Yamauchi H, Lind SE. Anticancer activity of the antibiotic clioquinol. Cancer Res. 2005 Apr 15; 65(8):3389-3395.

Dyk JC, Pieterse GM, Vuren JHJ. Histological changes in the liver of Oreochromis mossambicus (Cichlidae) after exposure to cadmium and zinc. Ecotoxicology and Environmental Safety; 2007; 66(3):432-440.

Foulkes EC, McMullen DM. Kinetics of transepithelial movement of heavy metals in rat jejunum. Am J Physiol 1987; 253:G134-G138.

Frederickson CJ. Neurobiology of zinc and zinc-containing neurons. Int Rev Neurobiol 1989; 131:145-238.

Frederickson, C.J., Suh, S.W., Koh, J.Y., Cha, Y.K., Thompson, R.B., LaBuda, C.J., Balaji, R.V. & Cuajungco, M.P. Depletion of intracellular zinc from neurons by use of an extracellular chelator in vivo and in vitro. J. Histochem Cytochem 2002; 50,1659-1662.

Frederickson CJ, Maret W, Cuajungco MP. Zinc and excitotoxic brain injury: a new model. Neuroscientist 2004; 10(1):18-25.

Gilmour P, Nyska A, Schladweiler MC, McGee JK, Wallenborn JG, Richards JH, Kodavanti UP. Cardiovascular and blood coagulative effects of pulmonary zinc exposure. Toxicology and Applied Pharmacology 2006; 211(1)41-52.

Gopal KV. Neurotoxic effects of mercury on auditory cortex networks growing on microelectrode arrays: a preliminary analysis. Neurotoxicology and Teratology 2002; 5526:1-8

Goyer RA, Clarkson TW. Toxic effect of metals, in Klaassen D. Curtis (ed): Casarett and Doull's Toxicology, 6th ed, Mc Graw-Hill, New York 2001 (pp. 812-814).

Gramowski A, Schiffmann D, Gross GW. Quantification of acute neurotoxic effects of trimethyltin using neuronal networks cultured on microelectrode arrays. NeuroToxicology 2000; 21:331-342.

Greger JL, Sickles VS. Saliva zinc levels: potential indicators of zinc status. Am J Clin Nutr 1979; 32:1859-1866.

Gross GW, Wen W, Lin J. Transparent indium-tin oxide patterns for extracellular, multisite recording in neuronal cultures. J Neurosci Meth 1985; 15:243-252.

Gross GW, Kowalski JM. Experimental and theoretical analyses of random network dynamics. In: Neural Networks, Concepts, Application and Implementation, Vol. 4, Antognetti P, Milutinovic V, editors. New Jersey:Prentice Hall, 1991 (pp. 47-110).

Gross GW, Schwalm FU. A closed chamber for long-term electrophysiological and microscopical monitoring of monolayer neuronal networks. J Neurosci Meth 1994; 52:73-85.

Gross GW. Internal dynamics of randomized mammalian neuronal networks in culture. In: Enabling Technologies for Cultured Neural Networks, Stenger DA, McKenna TM, editors. New York: Academic Press, 1994 (pp. 277-317).

Gross GW, Azzazy HME, Wu MC, Rhoades BK. The use of neuronal networks on multielectrode arrays as biosensors. Biososensors and Bioelectronics 1995; 10:553-567.

Gross GW, Pancrazio JPP. Neuronal Network Biosensors. In: Smart Biosensor Technology, Knopf GK, Bassi AS, editors. Marcel Dekker, Inc. 2006 (in press).

Gross GW, Gopal KV. Emerging histiotypic properties of cultured neuronal networks. In: Advances in Network Electrophysiology using Microelectrode Arrays, Taketani, editor. Kluwer Pulishing Co. 2006 (in press).

Gunshin H, Noguchi, T, Naito H. Effect of calcium on the zinc uptake by brush border membrane vesicles isolated from the rat small intestine. Agric Biol Chem 1991; 55:2813-2816.

Han Y, Wu SM. Modulation of glycine receptors in retinal ganglion cells by zinc. Proc Natl Acad Sci U S A. 1999; 96(6):3234-3238.

Harrison NL, Gibbons SJ. Zn^{2+}: an endogenous modulator of ligand and voltage gated ion channels. Neuropharm 1994; 33:935-952.

He LS, Yan XS, Wu DC. Age-dependent variation of zinc-65 metabolism in LACA mice. Int J Radiat Biol. 1991 Dec; 60(6):907-916.

Hempe JM, Cousins RJ. Cysteine-rich intestinal protein binds zinc during transmucosal zinc transport. Proc Natl Acad Sci U S A 1991; 88:9671-9674.

Hempe JM, Cousins RJ. Cysteine-rich intestinal protein and intestinal metallothionein: an inverse relationship as a conceptual model for zinc absorption in rats. J Nutr 1992; 122:89-95.

Hunt JR, Matthys LA, Johnson LK. Zinc absorption, mineral balance, and blood lipids in women consuming controlled lactoovovegetarian and omnivorous diets for 8 wk. Am J Clin Nutr 1998; 67:421-430.

Iitaka M, Kakinuma S, Fujimaki S, Oosuga I, Fujita T, Yamanaka K, Wada S, Katayama S. Induction of apoptosis and necrosis by zinc in human thyroid cancer cell lines. J Endocrinol. 2001 May; 169(2):417-424.

Istfan NW, Janghorbani M, Young VR. Absorption of stable70 Zn in healthy young men in relation to zinc intake. Am J Clin Nutr 1983; 38 :187-194.

IOM (Institute of Medicine). Dietary reference intakes for vitamin A, vitamin K, arsenic, boron, chromium, copper, iodine, iron, manganese, molybdenum, nickel, silicon, vanadium, and zinc. Washington, DC: National Academy Press 2001 (pp. 442-501).

Johnson PE, Hunt JR, Ralston NV. The effect of past and current dietary Zn intake on Zn absorption and endogenous excretion in the rat. J Nutr 1988; 118:1205-1209.

Kasper G, Weiser AA, Rump A, Sparbier K, Dahl E, Hartmann A, Wild P, Schwidetzky U, Castaños-Vélez E, Lehmann K. Expression levels of the putative zinc transporter LIV-1 are associated with a better outcome of breast cancer patients. Int J Cancer. 2005 Dec 20; 117(6):961-973.

Keefer EW, Norton SJ, Boyle NAJ, Talesa V, Gross GW. Acute toxicity screening of novel AChE inhibitors using neuronal networks on microelectrode arrays. NeuroTox 2001a; 22(1):3-12.

Keefer, EW, Gramowski, A., Stenger, D.A., Pancrazio, J.J., and Gross, G.W. Characterization of acute neurotoxic effects of trimethylolpropane phosphate via neuronal network biosensors. Biosensors and Bioelectronics 2001b; 16: 513-525.

Keefer EW, Gramowski, A., and Gross, G.W. NMDA receptor dependent periodic oscillations in cultured spinal cord networks. J. Neurophysiol. 2001c; 86: 3030-3042.

Kim YH, Kim EY, Gwag BJ, Sohn S, Koh JY. Zinc-induced cortical neuronal death with features of apoptosis and necrosis: mediation by free radicals. Neuroscience 1999; 89(1):175-182.

Knudsen E, Jensen M, Solgaard P. Zinc absorption estimated by fecal monitoring of zinc stable isotopes validated by comparison with whole-body retention of zinc radioisotopes in humans. J Nutr 1995; 125:1274-1282.

Koh JY, Choi DW. Zinc toxicity on cultured cortical neurons: involvement on Nmethyl-D-aspartate receptors. Neuroscience 1994; 60:1049-1057.

Koh JY, Suh SW, Gwag BJ, He YY, Hsu CY, Choi DW. The role of zinc in selective neuronal death after transient global cerebral ischemia. Science 1996; 272:1013-1016.

Lee DY, Brewer GJ, Wang YX. Treatment of Wilson's disease with zinc. VII. Protection of the liver from copper toxicity by zinc-induced metallothionein in a rat model. J Lab Clin Med 1989; 114:639-645.

Lin S, Tagliabracci VS, Chen X, Du Y. Albumin protects cultured cerebellar granule neurons against zinc neurotoxicity. Neuroreport 2005; 16(13):1461-1465.

Lucas JH, Czisny E, Gross GW. Adhesion of cultured mammalian CNS neurons to flame-modified hydrophobic surfaces. In Vitro 1986; 22:37-43.

Manev H, Kharlamov E, Uz T, Mason RP, Cagnoli CM. Characterization of zinc induced neuronal death in primary cultures of rat cerebellar granule cells. Exp Neurol 1997; 146:171-178.

Mantyh PW, Ghilardi JR, Rogers S, DeMaster E, Allen CJ, Stimson ER, Maggio JE. Aluminum, iron, and zinc ions promote aggregation of physiological concentrations of betaamyloid peptide. Journal of Neurochem 1993; 61(3):1171-1174.

Marin P, Israel M, Glowinski J, Premont J. Routes of zinc entry in mouse cortical neurons: role in zinc-induced neurotoxicity. Eur J Neurosci 2000; 12(1):8-18.

Methfessel AH, Spencer H. Zinc metabolism in the rat. I. Intestinal absorption of zinc. J Appl Physiol 1973; 34:58-62.

Morefield SI, Keefer EW, Chapman KD, Gross GW. Drug evaluations using neuronal networks cultured on microelectrode arrays. Biosensors and Bioelectronics 2000; 15:383-396.

Palmiter RD. The elusive function of metallothioneins. Proc. Natl. Acad. Sci. USA 1998; 95:8428-8430.

Prasad A, Schulert A, Sandstead H. Zinc, iron, and nitrogen content of sweat in normal and deficient subjects. J Lab Clin Med 1963; 62:84-89.

Ransom BR, Neale E, Henkart M, Bullock PN, Nelson PG. Mouse spinal cord in cell culture. I. Morphology and intrinsic neuronal electrophysiologic properties. J Neurophysiol 1977; 40(5):1132-1150.

Ravid BR, Rao KS. Role of metals in neuronal apoptosis: challenges associated with neurodegeneration. Curr Alzheimrt Res 2006; 3(4):311-326.

Richards MP, Cousins RJ. Mammalian zinc homeostasis: requirement for RNA and metallothionein synthesis. Biochem Biophys Res Commun 1975; 64:1215-1223.

Rivlin, RS. Misuse of hair analysis for nutritional assessment. Am J Med 1983; 75:489-493.

Rudolf E, Rudolf K, Cervinka M. Zinc induced apoptosis in HEP-2 cancer cells: the role of oxidative stress and mitochondria. Biofactors. 2005; 23(2):107-120.

Ruiz A, Walker M, Fabian-Fine R, Kullmann D. Endogenous Zinc Inhibits GABAA Receptors in a Hippocampal Pathway. J Neurophysiol 2004; 91:1091-1096.

Sandstrom B, Abrahamsson H. Zinc absorption and achlorhydria. Eur J Clin Nutr 1989;43:877-879.

Sensi SL, Canzoniero LMT, Yu SP, Ying H, Koh JY. Measurement of intracellular free zinc in living cortical neurons: routes of entry. J Neurosci 1997; 17(24):9554-9564.

Sensi SL, Yin HZ, Weiss JH. Glutamate triggers preferential Zn^{2+} flux through Ca^{2+} permeable AMPA channels and consequent ROS production. Neuroreport 1999; 10(8):1723-1727.

Sheline CT, Behrens MM, Choi DW. Zinc-induced cortical neuronal death: contribution of energy failure attributable to loss of NAD(+) and inhibition of glycolysis. J Neurosci 2000; 20(9):3139-3146.

Sheline CT, Ying HS, Ling CS, Canzoniero LM, Choi DW. Depolarization-induced 65zinc influx into cultured cortical neurons. Neurobiol Dis 2002; 10(1):41-53.

Smart TG, Xie X, Krishek BJ. Modulation of inhibitory and excitatory amino acid receptor ion channels by zinc. Prog Neurobiol 1994; 42:393-441

Spiridon M, Kamm D, Billups B, Mobbs P, Attwell D. Modulation by zinc of the glutamate transporters in glial cells and cones isolated from the tiger salamander retina. J Physiol 1998; 506 (Pt 2):363-376.

Suh SW, Koh JY, Choi DW. Extracellular zinc mediates selective neuronal death in hippocampus and amygdala following kainate-induced seizure. Soc Neurosci Abstr 1996; 22:2101.

Tacnet F, Watkins DW, Ripoche P. Studies of zinc transport into brush-border membrane vesicles isolated from pig small intestine. Biochim Biophys Acta 1990; 1024:323-330.

Talcott P, Peterson ME: Zinc Poisoning. In: Small Animal Toxicology. W. B. Saunders, Philadelphia, 2001 (pp. 756-761).

Taylor KM, Hiscox S, Nicholson RI. Zinc transporter LIV-1: a link between cellular development and cancer progression. Trends Endocrinol Metab 2004; Dec 15(10):461-463.

Uzzo RG, Leavis P, Hatch W, Gabai VL, Dulin N, Zvartau N, Kolenko VM. Zinc inhibits nuclear factor-kappa B activation and sensitizes prostate cancer cells to cytotoxic agents. Clin Cancer Res. 2002; Nov 8(11):3579-3583.

Vandenberg RJ, Mitrovic AD, Johnston GA. Molecular basis for differential inhibition of glutamate transporter subtypes by zinc ions. Mol Pharmacol 1998; 54(1):189-196.

Wastney ME, Aamodt RL, Rumble WF. Kinetic analysis of zinc metabolism and its regulation in normal humans. Am J Physiol 1986; 251:R398-R408.

Weiss JH, Sensi SL, Koh JY. Zn^2+: a novel ionic mediator of neural injury in brain disease. Trends Pharmacol Sci. 2000; 21:395-401.

Westbrook GL and Mayer ML. Micromolar concentrations of $Zn2^+$ antagonize NMDA and GABA responses of hippocampal neurons. Nature 1987; 328:640-643.

Xia Y, Gopal KV, Gross GW. Differential acute effects of fluoxetine on frontal and auditory cortex networks in vitro. Brain Research 2003; 973:151-160.

Xia Y, Gross GW. Histiotypic electrophysiological responses of cultured neuronal networks to ethanol. Alcohol 2003; 30:167-174.

Young Kyu Min, Jong Eun Lee and Kwang Chul Chung. Zinc induces cell death in immortalized embryonic hippocampal cells via activation of Akt-GSK-3ß signaling. Experimental Cell Research 2007; 313:(2)312-321.